Transport Properties of Chiral p-wave Superconductor-Normal Metal Nanostructures

Ahmet Keles

A dissertation
submitted in partial fulfillment of the
requirements for the degree of

Doctor of Philosophy

University of Washington

2014

Reading Committee:

Anton Andreev, Chair

Boris Spivak

David Cobden

Program Authorized to Offer Degree:
Physics

University of Washington

Abstract

Transport Properties of Chiral p-wave Superconductor-Normal Metal Nanostructures

Ahmet Keles

Chair of the Supervisory Committee:
Professor Anton Andreev
Department of Physics

In this thesis, we present a theory of electron transport for unconventional superconductors. We focus on the superconducting properties of Sr_2RuO_4, which is a strong candidate for two dimensional p-wave superfluidity in electronic systems. We present Green function formulation of the theory of superconductivity and reduce the formulation within quasiclassical approximation. To study the systems with disordered normal metal junctions, we derive the boundary conditions of quasiclassical equations from the microscopic theory considering a spin active boundary. Boundary between normal metal and superconductor is modeled with Rashba type spin orbit coupling. An exact solution of the resulting equations are given and the resistance of the model system is calculated as a function of temperature, boundary transparency and symmetry of the superconducting state. The developed theory is used to study the phase transition of unconventional superconductors with increasing impurity concentration. It has been shown that, in the strong disordered regime, system can be modeled as Mattis model known from the theory of spin glasses. We show that with increasing disorder there will be two consecutive phase transitions: A phase transition from unconventional superconductor to s-wave superconductor followed by a transition from s-wave superconductor to normal metal. A qualitative phase diagram is prsented and corrections to Mattis model approximation is considered.

TABLE OF CONTENTS

LIST OF FIGURES

ACKNOWLEDGMENTS

I would like to express my sincere appreciation to Boris Spivak and Anton Andreev for their support and patience during the years of my education at the University of Washington. I am thankful to Marcel den Nijs and Chris Laumann for many useful discussions. I am thankful to David Cobden for his kind interest in reading this thesis. I also would like to thank everyone I had a chance to talk to and learn from at the Physics Department at UW. I would like to thank my friends Altug Poyraz, Omer Yetemen, Onur Cem Namli, Egor Klevac for their invaluable company during my PhD studies. Finally I would like to thank my family; this work would not have been possible without their constant support.

Chapter 1

INTRODUCTION

1.1 A short history of superconductivity

The theory of superconductivity developed by Bardeen, Cooper and Schrieffer (BCS) in 1957[2] has been the solution of a fifty year puzzle that started with Kammerlingh Onnes' discovery of the phenomena[3] and immediately accepted by the physics community leading to Nobel prize in physics to its designers in 1972. The theory has been remarkably successful in explaining universal properties of early classical superconductors, like disappearance of resistance, Meissner effect, tunneling and Josephson effects and some other thermodynamic and electromagnetic properties (see [4, 5, 6, 7, 8] for introduction and experimental background). Later, this theory has been put in a more elegant canonical form by Bogoliubov[9] and Valatin[10], quantum field theoretical formulation was constructed by Gor'kov[11] and Nambu[12] and finally the theory was complete with Gor'kov's derivation of Ginzburg-Landau theory from BCS theory[13].

BCS theory is based on electron pairs (which are called Cooper pairs) bound together in a spin singlet, spherically symmetric s-wave orbital state glued through a phonon mediated attractive interaction that gives rise to a spectrum with fully isotropic gap on the Fermi surface. The theory was developed for electrons in conductors but shortly after BCS, questions regarding the possibility of this state in other quantum systems like liquid ^{3}He have arisen. In the case of ^{3}He, it was clear that BCS treatment of a possible pairing was not possible because strong hardcore repulsion of ^{3}He atoms disable s-wave pairing. This problem has lead Anderson and Morel[14] to the generalization of the BCS theory to Cooper pairs with higher angular momentum states which opened the era of unconventional superconductors. Shortly after Anderson and Morel, Balian and Werthamer proposed slightly different pairing symmetry which was thermodynamically more stable. In 1973 both of these predictions has been observed in the superfluid state of liquid ^{3}He below milikelvin temperatures. Today

these pairing symmetries are called A and B phases of the fermionic superfluid helium.

By the end of 70s, discovery of organic conductors and some so called heavy fermion compounds[15] added a new chapter to the problem of superconductivity. Since physics of these materials was dominated by strong electron interactions akin to the fermionic helium case, observation of superconductivity in these materials has been considered as a new realization of superconductivity with Cooper pairs in a non-zero angular momentum state. However situation has been realized to be much more complex due to existence of f orbital correlations and strong spin orbit coupling. After more than 30 years since their discovery, the symmetry of superconducting state in these materials is still controversial.

Surprising discovery of superconductivity in ceramic compound in 1986 by Bednorz and Muller in 1986[16] has been one of the biggest impacts of superconductivity in condensed matter physics. Because of their high transition temperatures they have received an immense amount of interest and they have been called high temperature superconductors. In the search for similar compounds with higher transition temperatures, superconductivity in Sr_2RuO_4 has been discovered in 1995[1]. This material has the same layered perovskite structure as high temperature superconducting materials and it has been the first compound that shows superconductivity without copper in this class of materials. Its low transition temperature, 1.5K°, had already signaled that there was something different about this material in compared to cuprates. Later, based on the fact that it was a strongly correlated Fermi liquid above its transition temperature similar to liquid ^{3}He in its normal state, it has been proposed to be two dimensional anolog of superfluid ^{3}He[17].

1.2 Disorder in superconductivity

Before discussing effect of disorder on the superconducting state, it is important to note that early classical superconductors are distinguished in two limits: In the first class of superconductors known as London superconductors (this class is also known as soft superconductors or type-I superconductos) characteristic scale of electromagnetic field denoted by λ is much bigger than the characteristic scale of Cooper pairs which is denoted by ξ. In this regime, electromagnetic response of the superconductor is determined through local London equations. In the second class of superconductors known as Pippard type super-

conductors (also known as hard superconductors or type-II superconductors) Cooper pair dimensions are bigger than the scale of electromagnetic field which gives rise to non-local response.

Effect of impurities can be very diverse on the superconducting state. First of all, it can be argued that with increasing disorder the initial change in the superconducting state occurs when when mean free path ℓ becomes such that Cooper pair dimension becomes order of penetration depth. After this point, superconductor transforms from Pippard type to London type. In this so called dirty superconductor regime, one can expect that superconducting correlations would survive until the mean free path becomes order of coherence length at which superconductivity will be destroyed.

This qualitative description is also observed in the experiments but it must be born in mind that the fate of superconductor with disorder depends on the nature of impurities and on the existence of an external electromagnetic field, but most importantly on the symmetry of the superconducting state. In conventional superconductors without external electromagnetic field, thermodynamic properties of the system shows very minute changes with non-magnetic impurities whereas magnetic impurities are detrimental to the superconducting state. It has been a curious observation since the early days of the discovery of superconductivity that transition temperatures of classical superconductors showed a small change with increasing non-nonmagnetic doping at around 1% concentration but after this point, in the dirty superconductor regime, almost no change occurs with higher concentrations up to 20% to 40% depending on the material. Also it must be noted that, in the presence of an external field, even non-magnetic impurities suppress classical superconductivity. In the case of unconventional superconductors, however, any doping - magnetic or nonmagnetic, with or without external field- has been observed to strongly suppress superconductivity.

One of the most important explanations of the effects of disorder on the superconducting state is done by Anderson by generalization of the BCS theory to systems with strong disorder, which is now known as Anderson's theorem[18]. Anderson's arguments are based on the empirical and qualitative discussions presented in above paragraphs. He basically showed that, one can construct a BCS theory based on the exact eigenstates of disordered

system and consider pairing with time reversal states. If the disorder does not break the time reversal state there will always be pairs of available scattering states for the initial cooper pair so that superconducting correlations will survive to arbitrarily higher disorder until $\xi \approx \ell$. In the case of a broken time reversal symmetry, this argument will lose its validity and superconductivity will be suppressed at much lower concentrations. Since pairs in unconventional superconductors are in a nonzero angular momentum state, they are not time reversal partners of each other and Anderson's theorem does not work for this class.

Field theoretical treatment of the dirty superconductor problem is formulated by Abrikosov and Gor'kov[19] which will be presented in Chapter 4. The basic idea is that, in the case of non-magnetic impurities, self-energy correction to normal Green function and anomalous Green function becomes proportional to each other which will only give rise to a rescaling of superconducting coherence length and the pairing will survive. In the case of a broken symmetry, this cancellation will not occur and superconductivity will be suppressed.

1.3 Superconductivity in Sr_2RuO_4

In this section, we give a summary of the most important properties of Sr_2RuO_4 for completeness. Further details can be obtained from [1, 20]. Sr_2RuO_4 is a strongly anisotropic material with layered perovskite crystal structure with tetragonal point group symmetry which is shown in Fig.1.1. It is a strongly correlated quasi two dimensional Fermi liquid above its transition temperature. Fermi surface consists of three two dimensional sheets due to three electrons in the $4d_{xy}$, $4d_{xz}$ and $4d_{yz}$ orbitals of ruthenium atoms as shown in Fig. 1.2. Quasi-one dimensional $d_{xz,yz}$ orbitals are α and β bands where they are hole-like and electron-like respectively. Two dimensional band due to d_{xy} orbital is called γ band and it is electron like. Experiments studying transport and thermodynamic properties of this material found metalic resistace, specific heat and spin susceptibility with mass and susceptibility enhancements of order of 10.

Superconducting phase transition takes place at a relatively low temperature which around 1.5K° for extremely clean samples. Although most experiments are in convergence to the indication of a spin triplet chiral p-wave superconductor, there are still controversies to be resolved before a final decision. Firs of all, the superconducting state is very sensitive

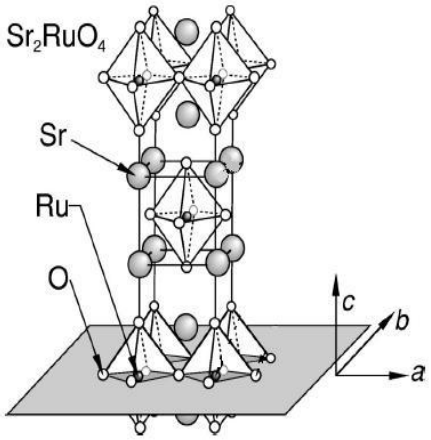

Figure 1.1: Crystal structure of Sr_2RuO_4. Highly conducting ruthanate layers are called ab planes whereas the orthogonal direction separating ruthenate layers with strontium is called c direction (Figure is from [1]).

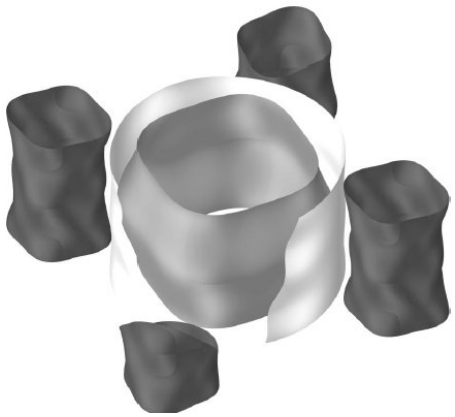

Figure 1.2: Fermi surface of Sr_2RuO_4. Black and grey sheets are called α an β sheets which are electron and hole like respectively. The white cylindrical sheet is called γ sheets which is hole like (Figure from [1]).

to doping with nonmagnetic impurities which is an indication of unconventional pairing. Spin susceptibility measurements by NMR Knight shift and polarized neutron scattering has shown no suppression of susceptibility below the transition point which showed the triplet spin part of the Cooper pairs. Finally Kerr rotation experiments has shown the broken time reversal symmetry in the superconducting phase[21]. Although there are numerous experiments indicating the conclusion of chiral p-wave order, there are still unsolved question. Among these puzzles, the strongest doubt comes from the absence of edge states and boundary magnetization which is related to so called angular momentum paradox of superfluid helium in its A-phase[22, 23, 24]. Although there are some proposals for the possible discrepancy[25], the absolute answer is still unknown.

1.4 Outline of the thesis and conclusions

In this thesis, we study effect of disorder on the superconducting state of unconventional superconductors in particular a chiral p-wave superconductor considering Sr_2RuO_4 as our system. The outline of the thesis as well as the important conclusions are summarized as follows:

In chapter 2, we are going to give a short summary of field theoretical formulation of disordered superconductors for the sake of completeness and notational consistency based on [26, 7]. After giving a general sketch of imaginary time Gor'kov Nambu formalism, we will consider real time Keldysh technique for studying transport in the quasiclassical formalism.

In chapter 3, we will set up the problem of disordered normal metal-chiral p-wave superconductor junction and calculate the resistance of the system. After derivation of spin dependent boundary conditions in the diffusive regime, we find that resistance of the junction depends strongly on the spin orbit couling at the boundary and the spin wavefunction orientation of the Cooper pairs that can be very useful for experimental verification of triplet superconductivity through tunneling.

In Chapter 4, we study unconventional superconductor-diffusive normal metal phase transition at zero temperature with increasing disorder withing mean field approximation and show that sytem is described by Mattis model, known from the theory of spin glasses.

As a result, we show that there will be two phase transitions as a function of increasing disorder: an unconventional superconductor to conventional s-wave superconductor followed by s-wave superconductor to diffusive normal metal.

Chapter 2

BCS THEORY AND NAMBU GORKOV FORMALISM

2.1 Gor'kov Equations

In this chapter we are going to summarize the basic ingredients of Gor'kov formulation that will be necessary for our discussion. Further details can be obtained from references [7, 26, 27]. Let us start with the general Hamiltonian

$$\begin{aligned} H &= \sum_{\mathbf{p}} \xi_{\mathbf{p}} \psi^{\dagger}_{\alpha}(\mathbf{p})\psi_{\alpha}(\mathbf{p}) \\ &+ \sum_{\mathbf{p},\mathbf{p}',\mathbf{q}} V_{\alpha\beta,\beta'\alpha'}(\mathbf{p},\mathbf{p}')\psi^{\dagger}_{\alpha}(-\mathbf{p}+\frac{\mathbf{q}}{2})\psi^{\dagger}_{\beta}(\mathbf{p}+\frac{\mathbf{q}}{2})\psi_{\beta'}(\mathbf{p}'+\frac{\mathbf{q}}{2})\psi_{\alpha'}(-\mathbf{p}'+\frac{\mathbf{q}}{2}). \end{aligned} \tag{2.1}$$

Here summation convention is implied for the spin indices which indicated by the Greek letters and fermionic operators satisfy the equal time anti-commutation relations,

$$\left\{\psi_{\alpha}(\mathbf{p},\tau),\psi^{\dagger}_{\beta}(\mathbf{p}',\tau)\right\} = \delta_{\alpha\beta}\delta(\mathbf{p}-\mathbf{p}') \tag{2.2a}$$

$$\left\{\psi_{\alpha}(\mathbf{p},\tau),\psi_{\beta}(\mathbf{p}',\tau)\right\} = \left\{\psi^{\dagger}_{\alpha}(\mathbf{p},\tau),\psi^{\dagger}_{\beta}(\mathbf{p}',\tau)\right\} = 0. \tag{2.2b}$$

Interaction potential is assumed to be attractive and should satisfy the following condition due to fermionic anticommutation:

$$V_{\alpha\beta,\beta'\alpha'}(\mathbf{p},\mathbf{p}') = -V_{\beta\alpha,\beta'\alpha'}(-\mathbf{p},\mathbf{p}') = -V_{\alpha\beta,\alpha'\beta'}(\mathbf{p},-\mathbf{p}') = V_{\beta\alpha,\alpha'\beta'}(-\mathbf{p},-\mathbf{p}'). \tag{2.3}$$

We perform a mean field decoupling on the quartic terms in Eq. (2.1) by using the following order parameter decoupling

$$\Delta_{\alpha\beta}(\mathbf{p},\mathbf{q}) = -\sum_{\mathbf{p}'} V_{\alpha\beta,\beta'\alpha'}(\mathbf{p},\mathbf{p}')\left\langle\psi_{\beta'}(\mathbf{p}'+\frac{\mathbf{q}}{2})\psi_{\alpha'}(-\mathbf{p}'+\frac{\mathbf{q}}{2})\right\rangle \tag{2.4a}$$

$$\Delta^{\dagger}_{\beta\alpha}(\mathbf{p},\mathbf{q}) = -\sum_{\mathbf{p}'} V_{\alpha'\beta',\beta\alpha}(\mathbf{p},\mathbf{p}')\left\langle\psi^{\dagger}_{\alpha'}(-\mathbf{p}'+\frac{\mathbf{q}}{2})\psi^{\dagger}_{\beta'}(-\mathbf{p}'+\frac{\mathbf{q}}{2})\right\rangle \tag{2.4b}$$

where $\langle ... \rangle$ represents average over Gibbs distribution. With this definition, one can obtain the following mean field Hamiltonian,

$$\begin{aligned} H &= \sum_{\mathbf{p}} \xi_{\mathbf{p}} \psi^{\dagger}_{\alpha}(\mathbf{p}) \psi_{\alpha}(\mathbf{p}) \\ &+ \frac{1}{2} \sum_{\mathbf{p},\mathbf{q}} \Delta_{\alpha\beta}(\mathbf{p},\mathbf{q}) \psi^{\dagger}_{\alpha}(-\mathbf{p}+\frac{\mathbf{q}}{2}) \psi^{\dagger}_{\beta}(\mathbf{p}+\frac{\mathbf{q}}{2}) + \Delta^{\dagger}_{\beta\alpha}(\mathbf{p},\mathbf{q}) \psi_{\beta}(\mathbf{p}+\frac{\mathbf{q}}{2}) \psi_{\alpha}(-\mathbf{p}+\frac{\mathbf{q}}{2}). \end{aligned} \tag{2.5}$$

We define the normal and anomalous Green functions in the usual way;

$$G_{\alpha\beta}(\mathbf{p},\mathbf{p}';\tau) = -\left\langle \mathcal{T} \psi_{\alpha}(\mathbf{p},\tau) \psi^{\dagger}_{\beta}(\mathbf{p}',0) \right\rangle \tag{2.6a}$$

$$F_{\alpha\beta}(\mathbf{p},\mathbf{p}';\tau) = \left\langle \mathcal{T} \psi_{\alpha}(\mathbf{p},\tau) \psi_{\beta}(-\mathbf{p}',0) \right\rangle \tag{2.6b}$$

$$F^{\dagger}_{\alpha\beta}(\mathbf{p},\mathbf{p}',\tau) = \left\langle \mathcal{T} \psi^{\dagger}_{\alpha}(-\mathbf{p},\tau) \psi^{\dagger}_{\beta}(\mathbf{p}',0) \right\rangle \tag{2.6c}$$

where $\mathcal{T}$ is the time ordering operator and τ is the imaginary time obtained from real time as $t \to -i\tau$ that satisfies $\tau \in [-1/T, 1/T]$ for temperature T. We assume that in static problems Green's functions only depend on the time difference τ. Fourier transform to frequency space representation can be written as

$$G_{\alpha\beta}(\mathbf{p},\mathbf{p}',\tau) = T \sum_{n=-\infty}^{\infty} G_{\alpha\beta}(\mathbf{p},\mathbf{p}',\omega_n) e^{-i\omega_n \tau} \tag{2.7}$$

where fermionic Matsubara frequencies are given by $\omega_n = (2n+1)\pi T$ and T is the temperature. Order parameter can be written in terms of anomalous Green functions as follows

$$\Delta_{\alpha\beta}(\mathbf{p},\mathbf{q}) = -T \sum_{n} \sum_{\mathbf{p}'} V_{\alpha\beta,\beta'\alpha'}(\mathbf{p},\mathbf{p}') F_{\beta'\alpha'}\left(\mathbf{p}'+\frac{\mathbf{q}}{2}, -\mathbf{p}'+\frac{\mathbf{q}}{2}\right) \tag{2.8a}$$

$$\Delta^{\dagger}_{\beta\alpha}(\mathbf{p},\mathbf{q}) = -T \sum_{n} \sum_{\mathbf{p}'} V_{\alpha'\beta',\beta\alpha}(\mathbf{p},\mathbf{p}') F^{\dagger}_{\beta'\alpha'}\left(\mathbf{p}'+\frac{\mathbf{q}}{2}, -\mathbf{p}'+\frac{\mathbf{q}}{2}\right). \tag{2.8b}$$

Time evolution of the field operators are obtained from the Heisenberg picture. In the imaginary time formalism, equation of motion can be written as

$$\frac{\partial \psi_{\alpha}(\mathbf{p},\tau)}{\partial \tau} = \left[H, \psi_{\alpha}(\mathbf{p},\tau)\right]. \tag{2.9}$$

Using this, the following set of equations of motion for the Green's functions can be obtained in a straightforward way;

$$(i\omega_n - \xi_{\mathbf{p}})\, G_{\alpha\beta}(\mathbf{p},\mathbf{p}';\omega_n) + \sum_{\mathbf{q}} \Delta_{\alpha\gamma}(\mathbf{p},\mathbf{q}) F^{\dagger}_{\gamma\beta}(\mathbf{p}-\mathbf{q},\mathbf{p}',\omega_n) = \delta(\mathbf{p}-\mathbf{p}')\delta_{\alpha\beta} \tag{2.10a}$$

$$(i\omega_n + \xi_{\mathbf{p}})\, F^{\dagger}_{\alpha\beta}(\mathbf{p},\mathbf{p}';\omega_n) + \sum_{\mathbf{q}} \Delta^{\dagger}_{\alpha\gamma}(\mathbf{p},\mathbf{q}) G_{\gamma\beta}(\mathbf{p}+\mathbf{q},\mathbf{p}',\omega_n) = 0 \tag{2.10b}$$

$$(i\omega_n - \xi_{\mathbf{p}})\, F_{\alpha\beta}(\mathbf{p},\mathbf{p}';\omega_n) - \sum_{\mathbf{q}} \Delta_{\alpha\gamma}(\mathbf{p},\mathbf{q}) G_{\gamma\beta}(-\mathbf{p}',-\mathbf{p}+\mathbf{q},-\omega_n) = 0. \tag{2.10c}$$

Note that we have explicitly preserved two momentum arguments in the Green functions to make it possible to consider impurity problems later. Near T_c, the order parameter Δ is small and anomalous Green functions can be expanded in powers of Δ. Then the following linearized self-consistency equation can be obtained,

$$\begin{aligned}\Delta_{\alpha\beta}(\mathbf{p},\mathbf{q}) = & - \quad T\sum_{n}\sum_{\mathbf{p}',\mathbf{p}'',\mathbf{q}'} V_{\beta\alpha\beta'\alpha'}(\mathbf{p},\mathbf{p}') G^{(0)}_{\beta'\alpha''}\left(\mathbf{p}'+\frac{\mathbf{q}}{2},\mathbf{p}''+\frac{\mathbf{q}'}{2};\omega_n\right) \\ & \times \quad G^{(0)}_{\alpha'\beta''}\left(-\mathbf{p}'+\frac{\mathbf{q}}{2},-\mathbf{p}''+\frac{\mathbf{q}'}{2};\omega_n\right)\Delta_{\alpha''\beta''}(\mathbf{p}'',\mathbf{q})\end{aligned} \tag{2.11}$$

Here $G^{(0)}$ is the Green function in the normal state taking all the external fields and perturbations which is the solution of systems of equations in 2.10a with taking $\Delta = 0$.

For a spatially homogeneous system, Green functions and order parameter depend only on momentums such that

$$G_{\alpha\beta}(\mathbf{p},\mathbf{p}';\omega_n) = G_{\alpha\beta}(\mathbf{p};\omega_n)\delta(\mathbf{p}-\mathbf{p}') \tag{2.12a}$$

$$F_{\alpha\beta}(\mathbf{p},\mathbf{p}';\omega_n) = F_{\alpha\beta}(\mathbf{p};\omega_n)\delta(\mathbf{p}-\mathbf{p}') \tag{2.12b}$$

$$\Delta_{\alpha\beta}(\mathbf{p},\mathbf{q}) = \Delta_{\alpha\beta}(\mathbf{p})\delta(\mathbf{q}). \tag{2.12c}$$

Thus, the set of equations in 2.10a takes a much simpler form as follows;

$$(i\omega_n - \xi_{\mathbf{p}})\, G_{\alpha\beta}(\mathbf{p},\omega_n) + \Delta_{\alpha\gamma}(\mathbf{p}) F^{\dagger}_{\gamma\beta}(\mathbf{p},\omega_n) = \delta_{\alpha\beta} \tag{2.13a}$$

$$(i\omega_n + \xi_{\mathbf{p}})\, F^{\dagger}_{\alpha\beta}(\mathbf{p},\omega_n) + \Delta^{\dagger}_{\alpha\gamma}(\mathbf{p}) G_{\gamma\beta}(\mathbf{p},\omega_n) = 0 \tag{2.13b}$$

$$(i\omega_n - \xi_{\mathbf{p}})\, F_{\alpha\beta}(\mathbf{p},\omega_n) - \Delta_{\alpha\gamma}(\mathbf{p}) G_{\gamma\beta}(-\mathbf{p},-\omega_n) = 0a. \tag{2.13c}$$

The set of algebraic equations in Eq. 2.13 can be solved to give;

$$G_{\alpha\beta}(\mathbf{p},\omega_n) = -\frac{i\omega_n + \xi_{\mathbf{p}}}{\omega_n^2 + \xi_{\mathbf{p}}^2 + |\Delta_{\mathbf{p}}|^2}\delta_{\alpha\beta} \qquad F_{\alpha\beta}(\mathbf{p},\omega_n) = \frac{\Delta_{\alpha\beta}(\mathbf{p})}{\omega_n^2 + \xi_{\mathbf{p}}^2 + |\Delta_{\mathbf{p}}|^2}. \tag{2.14}$$

In the normal state, the following Matsubara Green function can be obtained,

$$G^{(0)}_{\alpha\beta}(\mathbf{p},\omega_n) = \frac{\delta_{\alpha\beta}}{i\omega_n - \xi_{\mathbf{p}}}. \tag{2.15}$$

2.2 Nambu-Gor'kov Green Functions

The set of equations of motion in Eq. (2.10a) and their solutions can be written and solved in a more elegant way by use of a method due to Nambu [12] and Anderson [28]. To make a direct connection to the original reference we start with a singlet superconductor in the next section. We will later generalize it to triplet pairing.

2.2.1 Singlet Pairing

We start with singlet pairing BCS Hamiltonian within mean field approximation in momentum space taking $\mathbf{q} = 0$ in Eq. (2.1):

$$H = \sum_{\mathbf{p}} \xi_{\mathbf{p}} \psi^\dagger_\alpha(\mathbf{p})\psi_\alpha(\mathbf{p}) + \Delta(\mathbf{p})\psi^\dagger_\uparrow(\mathbf{p})\psi^\dagger_\downarrow(-\mathbf{p}) + \Delta^*(\mathbf{p})\psi_\downarrow(-\mathbf{p})\psi_\uparrow(\mathbf{p}) \tag{2.16}$$

where summation over spin label α is implied, $\xi_{\mathbf{p}}$ is single particle dispersion as before and $\Delta(\mathbf{p})$ is the singlet order parameter. Field operators ψ_α obey the fermionic anti-commutation relations as before. Following Nambu [12] we define the following spinor field in particle hole space, which is known as Nambu-spinor in the literature:

$$\Psi(\mathbf{p}) = \begin{pmatrix} \psi_\uparrow(\mathbf{p}) \\ \psi^\dagger_\downarrow(-\mathbf{p}) \end{pmatrix} \qquad\qquad \Psi(\mathbf{r}) = \begin{pmatrix} \psi_\uparrow(\mathbf{r}) \\ \psi^\dagger_\downarrow(\mathbf{r}) \end{pmatrix}. \tag{2.17}$$

Commutation relation for this field can be written as

$$\Big\{\Psi(\mathbf{p}), \Psi^\dagger(\mathbf{p}')\Big\} \equiv \begin{pmatrix} \{\psi_\uparrow(\mathbf{p}), \psi^\dagger_\uparrow(\mathbf{p}'\} & \{\psi_\uparrow(\mathbf{p}), \psi_\downarrow(-\mathbf{p}'\} \\ \{\psi^\dagger_\uparrow(-\mathbf{p}), \psi^\dagger_\uparrow(\mathbf{p}'\} & \{\psi^\dagger_\downarrow(-\mathbf{p}), \psi_\downarrow(-\mathbf{p}'\} \end{pmatrix} = \tau_0\delta(\mathbf{p}-\mathbf{p}'). \tag{2.18}$$

Here τ_0 is unit matrix in particle-hole space. Note that above equation can be considered as a definition of the anti-commutation for Nambu spinors if one gets confused about the order of matrix multiplication and the commutation brackets. BCS Hamiltonian in terms of Nambu spinor field can be written as,

$$H = \sum_{\mathbf{p}} \Psi^\dagger_{\mathbf{p}} \begin{bmatrix} \xi_{\mathbf{p}} & \Delta(\mathbf{p}) \\ \Delta^*(\mathbf{p}) & -\xi_{\mathbf{p}} \end{bmatrix} \Psi_{\mathbf{p}} + \text{const.} \tag{2.19}$$

where we will ignore the constant term in the sum from here on. Note that to get the above form we used the anti-commutation relation of electron field and the fact that $\xi_{\mathbf{p}} = \xi_{-\mathbf{p}}$ for quadratic dispersion. For convenience we define the following Hamiltonian density,

$$\mathcal{H} = \xi_{\mathbf{p}}\tau_3 + \hat{\Delta} \qquad\qquad \hat{\Delta} \equiv \begin{bmatrix} 0 & \Delta(\mathbf{p}) \\ \Delta^*(\mathbf{p}) & 0 \end{bmatrix} \tag{2.20}$$

so that Hamiltonian will have a more elegant form form

$$H = \sum_{\mathbf{p}} \Psi_{\mathbf{p}}^\dagger \mathcal{H} \Psi_{\mathbf{p}} \tag{2.21}$$

Equation of motion for the Nambu field can be obtained considering time dependence in Heisenberg picture as $\Psi(t) = e^{iHt}\Psi(0)e^{-iHt}$ as $i\partial_t\Psi = [\Psi, H]$. Calculating the commutation by using Eq. (2.20) and (2.21), one can get

$$i\frac{\partial\Psi}{\partial t} = \mathcal{H}\Psi \qquad\qquad i\frac{\partial\Psi^\dagger}{\partial t} = -\Psi^\dagger\mathcal{H}. \tag{2.22}$$

We define the time ordered Green function in the usual way in terms of Nambu field

$$\hat{G}(\mathbf{p}, t; \mathbf{p}', t') = -i\langle \mathcal{T}\Psi(\mathbf{r}, t)\Psi^\dagger(\mathbf{r}', t')\rangle \tag{2.23a}$$

$$\equiv \begin{bmatrix} -i\langle \mathcal{T}\psi_\uparrow(\mathbf{r}, t)\psi_\uparrow^\dagger(\mathbf{r}', t')\rangle & -i\langle \mathcal{T}\psi_\uparrow(\mathbf{r}, t)\psi_\downarrow(\mathbf{r}', t')\rangle \\ -i\langle \mathcal{T}\psi_\downarrow^\dagger(\mathbf{r}, t)\psi_\uparrow^\dagger(\mathbf{r}', t')\rangle & -i\langle \mathcal{T}\psi_\downarrow^\dagger(\mathbf{r}, t)\psi_\downarrow(\mathbf{r}', t')\rangle \end{bmatrix}, \tag{2.23b}$$

where time ordering operator $\mathcal{T}$ here should be considered after the outer products of spinors. In particular the second line above can be considered as a definition of the Nambu-Gor'kov time ordered Green function. To find the equation of motion for the Green function, one has to consider the jump in the Green function at $t = t'$ [29, chapter 2]. One can directly see that the off-diagonal elements do not have jump in the derivative since they are products of two creation or annihilation operators which always anti-commute. For $t = t'+0$, $\hat{G}_{11} = -i\langle\psi_\uparrow(\mathbf{r}, t)\psi_\downarrow(\mathbf{r}', t')\rangle$. For $t = t' - 0$, $\hat{G}_{11} = i\langle\psi^\dagger(\mathbf{r}', t')\psi(\mathbf{r}, t)\rangle$. Thus, the jump in the Green function at $t = t'$ can be found from the anti-commutation relation of electron fields as $\delta\hat{G}_{11} = \hat{G}_{11}(t + 0, t) - G_{11}(t - 0, t) = -i\delta(\mathbf{r}_1 - \mathbf{r}_2)$. Similarly one can also calculate the jump in the $\hat{G}_{22}$ and combine these the results to get $\delta\hat{G}(\mathbf{r}, t, \mathbf{r}', t') = -i\tau_0\delta(\mathbf{r} - \mathbf{r}')$. This jump should be added whenever one calculates the derivative of Nambu-Gor'kov Green

function with respect to time. Thus equation of motion for the Green function can be found by direct differentiation of the definition and using this jumps, which gives:

$$\left[i\frac{\partial}{\partial t} - \mathcal{H}\right] G(\boldsymbol{r}, t; \boldsymbol{r}', t') = \delta(\boldsymbol{r} - \boldsymbol{r}') \tag{2.24}$$

For a homogeneous system, we go to imaginary time and take Fourier transform with respect to imaginary time and space to get

$$\left[i\omega_n - \begin{pmatrix} \xi_{\mathbf{p}} & \Delta(\mathbf{p}) \\ \Delta^*(\mathbf{p}) & -\xi_{\mathbf{p}} \end{pmatrix}\right] G(\mathbf{p}, \omega_n) = 1 \tag{2.25}$$

Inverting the two by two matrix multiplying the Green function, one can easily find the matrix Green function as;

$$\hat{G}(\mathbf{p}, \omega_n) = \frac{1}{\omega_n^2 + \xi_{\mathbf{p}}^2 + |\Delta_{\mathbf{p}}|^2} \begin{bmatrix} -i\omega_n - \xi_{\mathbf{p}} & \Delta_{\mathbf{p}} \\ \Delta_{\mathbf{p}}^* & i\omega_n - \xi_{\mathbf{p}} \end{bmatrix} \tag{2.26}$$

which can be seen to be in agreement with the earlier result in Eq. (2.14).

2.2.2 General Pairing

In this section, we present the generalization of Gor'kov Nambu Green functions to general pairing, considering an application to triplet superconductors. In particular let us generalize the particle hole spinor to following form;

$$\Psi(\mathbf{p}) = \begin{pmatrix} \psi_\uparrow(\mathbf{p}) \\ \psi_\downarrow(\mathbf{p}) \\ \psi_\uparrow^\dagger(-\mathbf{p}) \\ \psi_\downarrow^\dagger(-\mathbf{p}) \end{pmatrix}, \qquad \Psi(\mathbf{r}) = \begin{pmatrix} \psi_\uparrow(\mathbf{r}) \\ \psi_\downarrow(\mathbf{r}) \\ \psi_\uparrow^\dagger(\mathbf{r}) \\ \psi_\downarrow^\dagger(\mathbf{r}) \end{pmatrix}. \tag{2.27}$$

Equal time anti-commutation relation for this 4 component field can be written as;

$$\{\Psi(\mathbf{p}), \Psi^\dagger(\mathbf{p}')\} = \delta(\mathbf{p} - \mathbf{p}') \tag{2.28}$$

To simplify the discussion we consider $\mathbf{q} = 0$ in Eq. (2.1) which can be written in the following matrix form:

$$H = \sum_{\mathbf{p}} \Psi^\dagger(\mathbf{p}) \begin{bmatrix} \hat{h}_0 & \hat{\Delta} \\ -\hat{\Delta}^* & -\hat{h}_0^T \end{bmatrix} \Psi(\mathbf{p}) \tag{2.29}$$

where $\hat{\Delta}$ is a two by two matrix in spin space as defined in Eq. (2.4) and we have used a generalized single particle Hamiltonian $\hat{h}_0$ which may contain disorder potential and spin orbit coupling for later applications. Here note that potential in the diagonal part transforms from particle-particle to hole-hole sector as $V \to -V^T$ where superscript T stands for matrix transposition.

At this point, we introduce the d-vector to simplify the notation of the Hamiltonian before we introduce the Green function. The anomalous Green function defined in Eq. (2.6) is product of two Fermi fields under time ordering operator. It is anti-symmetric under the exchange of these field operators due to time ordering operator which is a manifestation of Pauli exclusion principle. This anti-symmetric function can be written in terms of Pauli matrices in spin space as follows:

$$\hat{\Delta}(\mathbf{p}) = d_0(\mathbf{p}) i\hat{\sigma}_2 \qquad \text{singlet pairing} \tag{2.30}$$

$$\hat{\Delta}(\mathbf{p}) = \mathbf{d}(\mathbf{p}) \cdot \hat{\boldsymbol{\sigma}} i\hat{\sigma}_2 \qquad \text{triplet pairing} \tag{2.31}$$

where $d_0(\mathbf{p})$ has to be even whereas $\mathbf{d}(\mathbf{p})$ has to be odd in momentum $\mathbf{p}$ to satisfy the anti-symmetry. We also define the following form for the diagonal part $\hat{h} = h_0\sigma_0 + \mathbf{h} \cdot \sigma$ so that full Hamiltonian density for a generalized pairing can be written as

$$\mathcal{H} = \begin{bmatrix} h_0\sigma_0 + \mathbf{h} \cdot \sigma & (d_0\sigma_0 + \mathbf{d} \cdot \sigma) i\hat{\sigma}_2 \\ -i\hat{\sigma}_2(d_0^*\sigma_0 - \mathbf{d}^* \cdot \boldsymbol{\sigma}) & -h_0\sigma_0 + \mathbf{h}^* \cdot \boldsymbol{\sigma} \end{bmatrix} \tag{2.32}$$

Let us finish this section by giving the matrix structure of four by four Hamiltonian for a singlet and a triplet pairing superconductors:

For spin singlet s-wave pairing order parameter should have the form $\hat{\Delta} = \Delta_0 i\sigma_2$ where Δ_0 is a scalar which can be taken as real. Thus $d_0 = \Delta_0$ and $\mathbf{d} = 0$. Thus Hamiltonian density in momentum space will have the following form;

$$\mathcal{H}_{singlet} = \begin{bmatrix} \xi_{\mathbf{p}} & 0 & 0 & \Delta_0 \\ 0 & \xi_{\mathbf{p}} & -\Delta_0 & 0 \\ 0 & -\Delta_0 & -\xi_{\mathbf{p}} & 0 \\ \Delta_0 & 0 & 0 & -\xi_{\mathbf{p}} \end{bmatrix}. \tag{2.33}$$

It can be explicitly seen by looking at the eigenvalue of the matrix that we have the right spectrum; $\epsilon^2 = \xi_{\mathbf{p}}^2 + |\Delta_0|^2$. One can show that this form corresponds to BCS Hamiltonian

for singlet pairing which can be done by direct calculation of the term $\Psi^\dagger \mathcal{H} \Psi$.

For triplet p-wave pairing d-vector should be linear in $\mathbf{p}$ so we choose a general form $\mathbf{d} = \mathbf{A}\cdot\mathbf{p}$ where $A_{\mu j}$ is a rank-2 tensor (μ is Pauli spin matrix index and j is momentum component index) and $\mathbf{p} = -i\nabla$ with the complex conjugation $\mathbf{p}^* = i\nabla = -\mathbf{p}$. We need to be careful when we take the complex conjugate of order parameter and a safe way to do it is to write it in the above form. Then $\mathbf{d}^* = \mathbf{A}^* \cdot \mathbf{p}^* = -\mathbf{A}^* \cdot \mathbf{p}$. As an example let us choose the chiral p-wave order parameter which can be written as $\hat{\Delta} = (A_{1j} p_j \sigma_1)(-i\sigma_2)$ where we defined $\Delta_{\mathbf{p}} = A_{1j} p_j$. Chiral p-wave order parameter can be obtined form $(A_{1j}) = \Delta_0(1, i, 0)$ with all other components of tensor being zero. Note that p_j is unit vector. Also $A^*_{1j} = \Delta^*_0(1, -i, 0)$. Thus $[\Delta_{\mathbf{p}}]^* = -A^*_{1j} p_j = -\frac{\Delta_0}{p_F}(p_x - i p_y)$. Then Hamiltonian will have the following form:

$$\mathcal{H}_{triplet} = \begin{bmatrix} \xi_{\mathbf{p}} & 0 & \frac{\Delta_0}{p_F}(p_x + i p_y) & 0 \\ 0 & \xi_{\mathbf{p}} & 0 & \frac{\Delta_0}{p_F}(p_x + i p_y) \\ \frac{\Delta_0^*}{p_F}(p_x - i p_y) & 0 & -\xi_{\mathbf{p}} & 0 \\ 0 & \frac{\Delta_0^*}{p_F}(p_x - i p_y) & 0 & -\xi_{\mathbf{p}} \end{bmatrix} \tag{2.34}$$

Finding the spectrum and the corresponding Bogoliubov transformation is reduced to solving eigenvalue problem for a four by four matrix with this form. In the next section, we will further generalize the Green functions for non-equilibrium states by introducing the Kedysh technique in the quasiclassical approximation.

2.3 Keldysh Technique and Quasiclassical Green Functions

From the solution of imaginary time Green function, one can obtain the retarded and advanced real time Green function through usual analytical continuation procedure. These real time Green functions are defined through usual anti-commutator expectation values of Fermi field in the following way:

$$\hat{G}^R(\mathbf{r}, t; \mathbf{r}', 0) = -i\theta(t) \left\langle \left\{ \Psi(\mathbf{r}, t), \Psi^\dagger(\mathbf{r}', 0) \right\} \right\rangle, \tag{2.35a}$$

$$\hat{G}^A(\mathbf{r}, t; \mathbf{r}', 0) = i\theta(-t) \left\langle \left\{ \Psi(\mathbf{r}, t), \Psi^\dagger(\mathbf{r}', 0) \right\} \right\rangle, \tag{2.35b}$$

where hat over the Green functions indicate that they are four by four matrices in the spin and particle-hole space. This method gives a successful description of the physical systems in and close to equilibrium.

For systems far from equilibrium a diagrammatic perturbation theory is developed by Kedysh[30] which does not require analytical continuation to imaginary time. In this method, one has to consider so called Keldysh contour which is usual real time $t \in [-\infty, \infty]$ plus backwards time $t \in [\infty, -\infty]$. For details of this method, we refer to the original paper [30] and literature [31]. The central object of this method is matrix Green function in Keldysh space which has the following structure:

$$\check{G} \equiv \begin{bmatrix} \hat{G}^R & \hat{G}^K \\ 0 & \hat{G}^A \end{bmatrix}, \tag{2.36}$$

where we have used a check above the Green function in the Keldysh space which is the standard notation in the literature. Here the Keldysh component of the matrix Green function is defined in terms of commutator of the field operators as:

$$\hat{G}^K(\mathbf{r}, t; \mathbf{r}', 0) = -i \left\langle \left[\Psi(\mathbf{r}, t), \Psi^\dagger(\mathbf{r}', 0) \right] \right\rangle. \tag{2.37}$$

Here we note that it is important to consider the matrix structure of each elements of matrix Green functions in Eq. (2.36). Each element of this matrix is a four by four matrix in the Nambu-spin space.

It is possible to work out through the above scheme to obtain Gor'kov equations in this generalized Keldysh method but the result is more tedious and rarely needed for applications to real physical problems. In practice, Fermi wavelength, which is the scale of variation of the Green functions, is much smaller than the characteristic lengths of the many physical problems. For this reason, Green's functions pertain much more information than needed [32, 33]. Especially in the case of problems involving superconductivity, characteristic coherence length of Cooper pairs is much larger than inverse Fermi wave vector, i.e. $\xi \propto 1/t_c \gg 1/p_F$. In the quasiclassical method [34, 35, 36, 37], one integrates out all fine details of the Green's function by introducing the following quasiclassical Green function[38]:

$$\check{g}(\mathbf{x}, \mathbf{p}, \epsilon) = \frac{i}{\pi} \int d\xi_{\mathbf{p}} \int d^4x' e^{i\epsilon t' - i\mathbf{p}'\mathbf{r}} \tau_3 \check{G}(\mathbf{x}_1, \mathbf{x}_2) \tag{2.38}$$

where we have introduced $\mathbf{x}_1 = (t_1, \mathbf{r}_1)$ to simplify the notation, and defined center of mass $\mathbf{x} = (t, \mathbf{r}) = (\mathbf{x}_1 + \mathbf{x}_2)/2$ and relative $\mathbf{x} = (t', \mathbf{r}') = \mathbf{x}_1 + \mathbf{x}_2$ coordinates in the two point

Green function. In static problems, Green functions do not depend on the center of mass time so we will use the notation $\hat{g}(\mathbf{r}, \mathbf{p}, \epsilon)$ for quasiclassical green functions. Notice that the rapid oscillations of the Green function with the relative coordinates are integrated out and Green's function is integrated over single particle dispersion $\xi_{\mathbf{p}}$ which is the essence of this approximation.

To simplify the presentation here, we are going to assume an implicit singlet s-wave pairing and application of this technique to triplet case will be subject of Chapter 3. It can be shown starting from the Gor'kov equation for full Green function that quasiclassical Green function defined in Eq. (2.38) obeys the following transport-like equation

$$i\mathbf{v}_F \cdot \nabla \check{g} + [\epsilon \check{\tau}_3 + \check{\Delta} - \check{\Sigma}, \check{g}] = 0 \tag{2.39}$$

where $\mathbf{v}_F = \mathbf{p}_F/m$ is the Fermi velocity vector. Here $\hat{\Sigma}$ and $\hat{\Delta}$ are diagonal and off-diagonal self energies in the particle-hole subspace. Self-consistency equation for superconducting gap can be written within the quasiclassical approximation as [32, 38]:

$$\hat{\Delta}(\mathbf{p}, \mathbf{r}) = \int \frac{d\Omega_{\mathbf{p}'}}{4\pi} \int \frac{d\epsilon}{2\pi i} V(\mathbf{p}, \mathbf{p}') \left[\hat{g}^K(\mathbf{r}, \mathbf{p}', \epsilon)\right]_{o.d.} \tag{2.40}$$

where "o.d." means that one should consider the off-diagonal component of the Green function in the particle-hole space, which is also called anomalous component and $V(\mathbf{p}, \mathbf{p}')$ is two particle interaction which is assumed to be attractive in the BCS approximation. In our presentation, we are exclusively interested in the disordered systems. In this regard, diagonal self-energy in Eq. (2.39) can be written in the Born approximation as follows

$$\hat{\Sigma}(\mathbf{r}, \epsilon) = -\frac{i}{2\tau_e} \int \frac{d\Omega_{\mathbf{p}}}{4\pi} \hat{g}(\mathbf{r}, \mathbf{p}, \epsilon) \tag{2.41}$$

where τ_e is the scattering time from the point like non-magnetic impurities.

Finally, it must be noticed that Eilenberger equation is homogeneous whereas the underlying Gor'kov equations are inhomogeneous. This means that some information is lost regarding the normalization of the Green function, since if $\hat{g}$ is a solution of Eilenberger equation, so is $\hat{g}^2$. This situation can be fixed by considering the set of equations in homogeneous, equilibrium case which gives the following normalization constraint:

$$\check{g}^2 = 1 \tag{2.42}$$

which can be spelled out in the Keldysh space as follows:

$$\hat{g}^R\hat{g}^R = \hat{g}^A\hat{g}^A = 1 \tag{2.43a}$$

$$\hat{g}^R\hat{g}^K + \hat{g}^K\hat{g}^A = 0 \tag{2.43b}$$

where the Eq. (2.43b) is satisfied for any function of the form

$$\hat{g}^K = \hat{g}^R\hat{h} - \hat{h}\hat{g}^A \tag{2.44}$$

where $\hat{h}$ is an arbitrary function but it will be chosen to be of the following form [36]

$$\hat{h} = f_0\hat{\tau}_0 + f_1\hat{\tau}_3 \tag{2.45}$$

where it must be remembered that we use $\hat{\tau}$ for Pauli matrices in the particle-hole space.

Further details on the manipulation of Eq. (2.39) will be given in Chapter 3 for a specific application to p-wave superconductor. We close this section by giving the solution of Eilenberger equation for a homogeneous singlet superconductor to make connection with our earlier result in Eq. (2.14)

For a homogeneous system in equilibrium, gradient term in Eq. (2.39) will give zero and the remaining equation will be of simple algebraic form. Although it is quite straightforward to work out the calculations in the presence of impurity scattering self-energy, we also ignore this term here for simplicity by considering a clean s-wave superconductor. Order parameter for a singlet superconductor will give the following structure in the Keldysh and particle-hole space

$$\check{\Delta} = \begin{bmatrix} \hat{\Delta} & 0 \\ 0 & \hat{\Delta} \end{bmatrix}, \quad \hat{\Delta} = \begin{bmatrix} 0 & \Delta_0 i\hat{\sigma}_2 \\ \Delta_0^* i\hat{\sigma}_2 & \end{bmatrix}, \tag{2.46}$$

where the factor of $\hat{\tau}_3$ in the definition of quasiclassical Green function in Eq. (2.38) should be remembered when writing this form. Plugging this in Eq. (2.39) by taking gradient and impurity self-energy to be zero and solving the resulting equation, one can obtain

$$\hat{g}^R_{singlet} = \frac{1}{\sqrt{\epsilon^2 - |\Delta_0|^2}} \begin{bmatrix} \epsilon\hat{\sigma}_0 & \Delta_0 i\hat{\sigma}_2 \\ \Delta_0^* i\hat{\sigma}_2 & -\epsilon\hat{\sigma}_0 \end{bmatrix} \tag{2.47}$$

which can be shown to be consistent with Eq. (2.14) after $\xi_{\mathbf{p}}$ integration and properly taking analytical continuation to real frequecies. Advanced component can be obtained to be $\hat{g}^A = -\hat{\tau}_3(\hat{g}^R)^\dagger\hat{\tau}_3$ from the definitions Eq. (2.35) and (2.38).

2.4 Dirty Limit: Usadel Equation

At small temperatures, excitation energies or at strong disorder in which the condition $1/\tau_e \gg \epsilon, \Delta_0$ satisfied, momentum loses its meaning to be a good quantum label. Although the magnitude of momentum is still p_F set by Fermi surface, its direction is randomized because of strong impurity scattering in this regime. In this limit, it is reasonable to talk about a formulation averaged over momentum directions on the Fermi surface which is done through the Usadel Formulation[39]. Usadel Green function is defined as

$$\check{G}(\mathbf{r},\epsilon) = \int \frac{d\Omega_{\mathbf{p}}}{4\pi} \check{g}(\mathbf{r},\mathbf{p},\epsilon), \tag{2.48}$$

where we have used the uppercase G for Usadel Green function. The distinction between this quantity and the original Gor'kov-Nambu Green functions can be seen from the arguments of the function: Usadel Green functions depend on the position and the excitation energy. Corresponding equation of motion can be obtained from Eilenberger equation in 2.39 by substituting 2.48 with a small momentum dependent correction and perturbatively treating the terms of the same order which gives the following Usadel equation:

$$D\nabla\left(\check{G}(\mathbf{r},\epsilon)\nabla\check{G}(\mathbf{r},\epsilon)\right) + \left[i\epsilon\check{\tau}_3 + \check{\Delta}, \check{G}(\mathbf{r},\epsilon)\right], \tag{2.49}$$

where $D = v_F\ell/3$ is the diffusion constant in 3D and $\ell = v_F\tau_e$ is the mean free path. It can be seen that this form is particularly useful in a disordered normal metal in contact with a superconductor since the condition $\Delta = 0$ in a normal metal greatly simplifies the problem. In this case, solution of second order differential equation in Eq. (2.49) should be supplemented with the boundary conditions which will be the subject of the next section.

2.5 Boundary Conditions

Quasiclassical theory of superconductivity outlined above is based on the fact that characteristic scale of the variation is much larger than atomic seperation. It has been implicitly assumed in the derivation that two point Green functions are slowly varying quantities with the center of mass coordinates. In the presence of a boundary which separates to distinct materials where each side can be a superconductor or a normal metal, assumptions that

lead to quasiclassical theory lose their validity. The point is that near the boundary the variations can be as sharp as atomic dimension and the Green functions depend strongly on the center of mass variables.

However, quasiclassical theory can still be used in the presence of a boundary by supplementing the set of equations with phenomenological boundary conditions that connects the two sides of the barrier. For the case of a boundary without spin or magnetic activity, these boundary conditions are derived from the microscopic theory by Zaitsev[40]. Assuming a planar boundary on the xy-plane that separates two distinct regions $z > 0$ and $z < 0$, these boundary conditions can be written in the following form:

$$\check{g}_a(z_+, \mathbf{p}) = \check{g}_a(z_-, \mathbf{p}') \equiv \check{g}_a(0) \tag{2.50a}$$

$$\check{g}_a(0)\left[R\left(\check{g}_s^+(0)\right)^2 + \left(\check{g}_s^-(0)\right)^2\right] = T\check{g}_s^-(0)\check{g}_s^+(0) \tag{2.50b}$$

where $z_\pm$ means $z = \pm 0$ and Green functions with subscripts and superscripts in these equations are defines in the following way

$$\check{g}_{s,a}(z, \mathbf{p}) = \frac{\check{g}(z, \mathbf{p}_{in}) \pm \check{g}(z, \mathbf{p}_{out})}{2} \tag{2.51a}$$

$$\check{g}_s^\pm(0) = \frac{\check{g}_s(z_+, \mathbf{p}) \pm \check{g}_s(z_-, \mathbf{p})}{2} \tag{2.51b}$$

where $\mathbf{p}_{in}$ and $\mathbf{p}_{out}$ are incident and outgoing momentums with respect to the boundary. Note that we have dropped the obvious ϵ dependence of the Green functions in these boundary conditions for notational simplicity. T and R are transmission and reflection probabilities of the boundary layer determined by the transparency of the barrier.

Note that Zaitsev's boundary conditions are momentum dependent. In the case of strong disorder these boundary conditions can be simplified to get corresponding boundary conditions for Usadel formalism which is obtained by Kuprianov and Lukichev [41] in the following form

$$D\left[\check{G}(z)\frac{d\check{G}(z)}{dz}\right]_{z=\pm 0} = t\left[\check{G}(z_+), \check{G}(z_-)\right], \tag{2.52}$$

where $t = \langle v_F \cos\theta T/4R\rangle$. $\langle ...\rangle$ here means angular averaging over the Fermi surface and angle θ is the angle between momentum and the normal vector of the boundary so that $\mathbf{p}_\perp = p_F \cos\theta$.

Although boundary conditions in Eq. (2.51) and (2.52) are sufficient for most problems, they are not applicable to boundaries with spin activity. In this thesis, we are especially interested in boundaries in which spin orbit coupling is important. We will use Rashba type spin orbit coupling along the boundary so that, total potential along the boundary can be modelled in the following way

$$V(\mathbf{r}) = u\sigma_0 + u_{so}\mathbf{p} \times \hat{n} \cdot \sigma \tag{2.53}$$

Corresponding transmission matrix in the Gor'kov-Nambu space can be written in the following way:

$$T = t\hat{\tau}_3 + t_{so}\hat{\gamma} \tag{2.54}$$

where we defined the matrix $\hat{\gamma}$ as

$$\hat{\gamma} = \hat{\gamma}^\dagger = \begin{pmatrix} \mathbf{p} \times \hat{n} \cdot \sigma & 0 \\ 0 & -\mathbf{p} \times \hat{n} \cdot \sigma \end{pmatrix}.$$

We assume a low transparency barrier so that the reflection matrix $R \approx 1$ and $t, t_{so} \ll 1$ and also spin orbit coupling is small $t_{so} \ll t$. Boundary condition derived by Millis *et al.*[42] are

$$\check{g}^r_{out} - R'\check{g}^r_{in}R'^{-1} = -\frac{i}{2\pi}[T'(\check{g}^\ell_{in} + i\pi)T'^\dagger, \check{g}^r_{out}], \tag{2.55}$$

$$\check{g}^\ell_{in} - R^{-1}\check{g}^\ell_{out}R = -\frac{i}{2\pi}[\check{g}^\ell_{in}, T^\dagger(\check{g}^r_{out} + i\pi)T], \tag{2.56}$$

where $\check{g}^{r(l)}_{in}$ is the Eilenberger Green function on the right (left) side of the junction depending on a momentum vector coming into the boundary and $\check{g}^{r(l)}_{out}$ is the same function with a momentum direction out of the boundary.

In the Eilenberger equation, for strong perturbations along the boundary one can ignore ϵ and Δ so that;

$$i\mathbf{v}_F \cdot \nabla\check{g} - [\check{\sigma}, \check{g}] = 0 \tag{2.57}$$

$\check{\sigma}$ is the self energy coming from impurity scattering, in born approximation $\check{\sigma} = -i\langle\check{g}\rangle/2\tau$, where $\langle\rangle$ is average over solid angle in momentum space.

To first order in the transmission amplitude we make the approximation $R^{-1}\check{g}^\ell_{out}R \approx \check{g}_{out}$. We also define symmetric and antisymmetric in momentum p_z as $\check{g}_{s,a} = (\check{g}_{in} \pm \check{g}_{out})/2$.

Thus left hand side of Eq. (2.55) and (2.56) will be equal to $\check{g}_a$ to lowest order in transmission amplitude. In the same order of accuracy, we replace $\check{g}^r_{out} \approx \check{g}^r_s$ on the right hand side of Eq. (2.55) and $\check{g}^\ell_{in} \approx \check{g}^\ell_s$ on the right hand side of Eq. (2.56). With these approximations, Eq. (2.55) can be put into the form:

$$\check{g}^r_a = -\frac{i}{2\pi} t^2 [\check{g}^\ell_{in}, \check{g}^r_s] - \frac{i}{2\pi} t\delta t [\{\check{\gamma}, \check{g}^\ell_{in}\}\check{g}^r_s]. \tag{2.58}$$

Following the procedure used by Kuprianov and Lukichev, we multiply both sides of above equation with $p_z/p \equiv \cos\theta_{\mathbf{p}}$ and take angular average. On the right hand side we will have $\langle \cos\theta_{\mathbf{p}} \check{g}^r_a \rangle$. To find this average, we use Eilenberger equation ignoring ϵ and Δ within a range of mean free path ℓ around boundary which gives two equations in the form

$$2\ell_e \cos\theta_{\mathbf{p}} \partial \check{g}_a = \check{g}_s \langle \check{g}_s \rangle - \langle \check{g}_s \rangle \check{g}_s, \tag{2.59}$$

$$2\ell_e \cos\theta_{\mathbf{p}} \partial \check{g}_s = \check{g}_a \langle \check{g}_s \rangle - \langle \check{g}_s \rangle \check{g}_a. \tag{2.60}$$

Taking angular average of Eq. (2.59), one can see that $\langle \cos\theta_{\mathbf{p}} \check{g}_a \rangle$ is constant. Value of this constant can be found by multiplying both sides with $\cos\theta_{\mathbf{p}}$, taking average of both sides in Eq. (2.60) and using the normalizations $\check{g}_s^2 = 1$, $\{\check{g}_s, \check{g}_a\} = 0$. This gives $\langle \cos\theta_{\mathbf{p}} \check{g}^r_a \rangle = \frac{1}{3}\ell \check{g}_s \partial \check{g}_s$. Finally, we multiply both sides of Eq. (2.58) with $\mathbf{v}_F = v_F \cos\theta_{\mathbf{p}}$ and take angular average, which gives;

$$D\check{g}^r_s \partial \check{g}^r_s = t_1 [\langle \check{g}^\ell_{in} \rangle, \check{g}^r_s] + t_2 [\langle \{\check{g}^\ell_{in}, \check{\gamma}\} \rangle, \check{g}^r_s] \tag{2.61}$$

We assumed an order parameter on the left hand side such that Eilenberger Green function depends only on azimuthal angle $\varphi_{\mathbf{p}}$. This assumption is sufficuent to treat layered unconventional superconductors. This enables the seperation of $\varphi_{\mathbf{p}}$ and $\theta_{\mathbf{p}}$ integrals as, $\langle \check{g}^\ell_{in} \rangle = \int \frac{d\varphi_{\mathbf{p}}}{2\pi} \check{g}^\ell_{in}$, $\langle \{\check{g}^\ell_{in}, \check{\gamma}\} \rangle = \int \frac{d\varphi_{\mathbf{p}}}{2\pi} \{\check{g}^\ell_{in}, \check{\gamma}\}$ and we defined $t_1 = \int \frac{d\cos\theta_{\mathbf{p}}}{2} (-\frac{i}{2\pi} t^2 v_F \cos\theta_{\mathbf{p}})$, $t_2 = \int \frac{d\cos\theta_{\mathbf{p}}}{2} (-\frac{i}{2\pi} t\delta t v_F \cos\theta_{\mathbf{p}})$. It is clear that Eq. (2.61) is consistent with Kuprianov *et al.* for non magnetic boundary $t_2 = 0$.

In the next chapter, we present applications of quasiclassical theory derived here to the problem of p-wave superconductor-normal metal junction and consider the boundary problem in more detail.

Chapter 3

NORMAL METAL P-WAVE SUPERCONDUCTOR JUNCTION

Originally published as: A. Keles, A.V. Andreev, B.Z. Spivak "Electron transport in p-wave superconductor-normal metal junctions" Physical Review B, 89, 014505 (2014).

Electron transport in superconducting systems is very different from that in normal metals. Roughly speaking, the characteristic size of wave packets which carry current in metals is of the order of the Fermi wave length $\hbar/p_F$, while their charge is equal to the electron charge e. Here p_F is the Fermi momentum. On the other hand, the quasiparticle wave packets are coherent superpositions of electrons and holes. This results in a characteristic size of the wave packets which is much larger than $\hbar/p_F$. The charge of the packets depends on the energy and can be very different from the electron charge e. This has important consequences in electronic transport properties of superconductor-insulator-normal metal junctions.

3.1 Introduction

Transport properties of s-wave superconductor-insulator-normal metal junctions have been the subject of intensive experimental and theoretical research for decades, see for example, Refs. [43, 44, 45, 46, 47, 48]. In this case the Cooper pairs can be constructed from the two single particle wave functions related by a time reversal operation. At low temperatures the characteristic size of wave packets which carry current in the metal near the boundary is of the order of the normal metal coherence length $L_T = \sqrt{D/T}$, which turns out to be much larger than the elastic mean free path l. Here D is the diffusion coefficient, and T is the temperature. One of the consequences of the large size of the wave packets is that, in the presence of a current through the junction, the drop of the gauge-invariant potential Φ is pushed to distances of order L_T away from the boundary, which is much larger than both the thickness of the insulator and the elastic mean free path l. This is quite different from

the case of normal metal-insulator-normal metal junctions, where most of the potential drop occurs at the insulator.

In this article we develop a theory of electron transport in p-wave superconductor-insulator-normal metal junctions. The best known example of a p-wave superfluid is superfluid ^3He. One of the leading candidates for p-wave pairing in electronic systems is Sr_2RuO_4. There are numerous pieces of experimental evidence that the superconducting state of this material has odd parity, breaks time reversal symmetry and is fully gaped.[49, 50, 21, 51, 1, 20] One of the simplest forms of the order parameter which satisfies these requirements is the chiral p-wave state $\Delta(\mathbf{p}) \sim p_x \pm ip_y$, which has been suggested in Ref. [17]. It is a two-dimensional analog of superfluid $^3He - A$.[14] Another interesting scenario for the order parameter was suggested in Ref. [25]. Chirality of the pairing wave function leads to edge states and spontaneous surface currents. While the quasiparticle tunneling spectroscopy[52, 53, 54] confirmed the existence of the subgap states, the experiments in Ref. [23] did not confirm the existence of the edge supercurrent. (See Ref. [22] for a discussion about about consistency of the chiral p-wave phase for Sr_2RuO_4.) We think that electron transport experiments may clarify the situation.

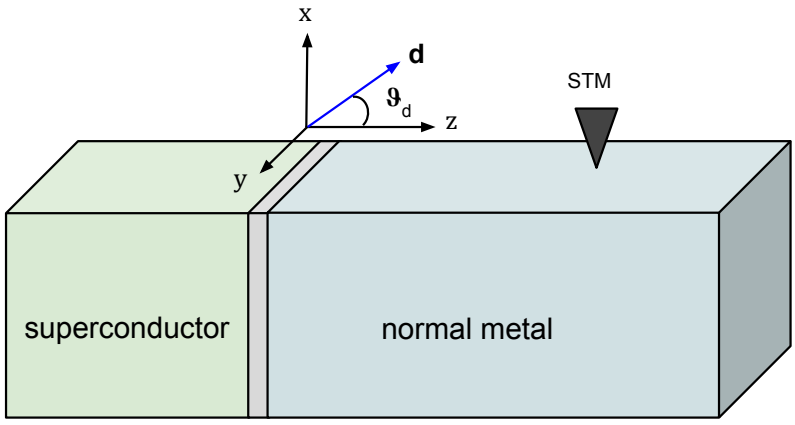

Figure 3.1: (color online) Schematic representation of the superconductor- insulator-normal metal junction. The vector $\hat{z}$ is along the c-axis of crystal, and $\vartheta_{\mathbf{d}}$ denotes the angle between spin vector $\mathbf{d}$ and $\hat{z}$. The dependence of the voltage inside the normal metal on the distance from the boundary may be measured by a scanning tunneling microscope (STM).

In this article we consider a p-wave superconductor-insulator-normal metal junction in the geometry in which the insulating boundary (xy-plane) is perpendicular to the c-axis of the layered chiral p-wave superconductor, as shown in Fig. (3.1). Although for simplicity we take the order parameter in the superconductor in the form[14, 7]

$$\hat{\Delta}(\mathbf{n}) = \Delta(\mathbf{n})(\mathbf{d}\cdot\boldsymbol{\sigma})i\sigma_2, \quad \Delta(\mathbf{n}) = \Delta_0 e^{i\varphi_{\mathbf{n}}}, \tag{3.1}$$

our results also apply to more complicated forms of the order parameter, such as for example that in Ref. [25]. Here $\mathbf{n}$ is a unit vector in the xy-plane, which points along $\mathbf{p}$, and $\varphi_{\mathbf{n}}$ is the azimuthal angle characterizing its direction $\mathbf{n} = (\cos\varphi_{\mathbf{n}}, \sin\varphi_{\mathbf{n}})$.

At temperatures well below the gap, tunneling of single electrons from the metal to the superconductor is forbidden. Thus, similar to the s-wave case, the resistance of the junction is determined by the tunneling of the electron pairs. Coherent pair tunneling gives rise to coherence between electrons and holes inside the normal metal. Electron-hole coherence in the metal is characterized by the anomalous Green function. The crucial difference between the s-wave and the p-wave cases is the following. In the p-wave case in the absence of spin-orbit interaction only the p-wave component is induced inside the normal metal. The latter is exponentially suppressed at distances larger than l away from the superconductor-normal metal boundary. As a result, in the diffusive regime the conductance of the junction is significantly suppressed. In the presence of the spin-orbit interaction the p-wave order parameter in the superconductor is partially converted to the s-wave component inside the normal metal. At low temperatures, the s-wave component propagates into the metal to large distances from the boundary. Consequently, it is this component that determines the low temperature resistance of the system.

We show below that Rashba-type spin-orbit coupling at the boundary between the normal metal and the p-wave superconductor leads to strong dependence of the resistance on the direction of the vector $\mathbf{d}$, which characterizes the spin structure of the order parameter in Eq. (3.1). Since the spin orientation of the order parameter may be controlled by an external magnetic field[55] our predictions may be tested in experiment. Qualitatively, this dependence may be understood as follows. In our geometry (with the z-axis parallel to the c-axis of the crystal) the z-component of the total (orbital plus spin) angular momentum,

$J_z = L_z + s_z$, is conserved during tunneling even in the presence of spin-orbit interaction. Therefore the s-wave singlet proximity effect in the normal metal is produced only by the pairs with $J_z = 0$ in the p-wave superconductor. Since in our geometry the z-component of the orbital angular momentum in a $p_x + ip_y$ superconductor is $L_z = +1$ we conclude that only the part of the condensate with $s_z = -1$ induces the s-wave proximity effect in the normal metal. This condensate fraction corresponds to the the components of the vector $\mathbf{d}$ lying in the xy-plane.

3.2 Kinetic scheme for description of electron transport in p-wave superconductor-normal metal junctions.

The conventional description of the electronic transport in superconductors based on the Boltzmann kinetic equation is valid when all spatial scales in the problem, including the mean free path l, are larger than the characteristic size of electron wave packets. At low temperatures, $L_T \gg l$, this condition is violated and this approach cannot be used for the description of the effects mentioned above.

The set of equations describing the electronic transport in s-wave superconductors in this situation has been derived in Ref. [36]. Below we review a modification of this approach for the case where the superconducting part of the junction is a p-wave superconductor. The central object of this approach is the matrix Green function in the Keldysh space

$$\check{G}(\mathbf{x}_1;\mathbf{x}_2) = \begin{pmatrix} \hat{G}^R & \hat{G}^K \\ 0 & \hat{G}^A \end{pmatrix}. \tag{3.2}$$

The retarded, advanced and Keldysh Green functions in this equation can be written in the following form

$$\hat{G}^R_{\ell\ell'}(\mathbf{x}_1;\mathbf{x}_2) = -i\theta(t_1 - t_2)\langle\{\psi_\ell(\mathbf{x}_1), \psi^\dagger_{\ell'}(\mathbf{x}_2)\}\rangle, \tag{3.3}$$

$$\hat{G}^A_{\ell\ell'}(\mathbf{x}_1;\mathbf{x}_2) = i\theta(t_2 - t_1)\langle\{\psi_\ell(\mathbf{x}_1), \psi^\dagger_{\ell'}(\mathbf{x}_2)\}\rangle, \tag{3.4}$$

$$\hat{G}^K_{\ell\ell'}(\mathbf{x}_1;\mathbf{x}_2) = -i\langle[\psi_\ell(\mathbf{x}_1), \psi^\dagger_{\ell'}(\mathbf{x}_2)]\rangle. \tag{3.5}$$

Here $\mathbf{x} = (\mathbf{r}, t)$ denotes the space-time coordinate, and the indices $\ell, \ell' = 1...4$ label the four components of the fermion operator in the Nambu/spin space; $\psi_1 = \psi_\uparrow$, $\psi_2 = \psi_\downarrow$,

$\psi_3 = \psi_\uparrow^\dagger$, $\psi_4 = \psi_\downarrow^\dagger$. Finally, the anticommutator and the commutator of operators A and B are denoted by $\{A, B\}$ and $[A, B]$ respectively.

Introducing the new variables, $\mathbf{x} = (\mathbf{r}, t) = (\mathbf{x}_1 + \mathbf{x}_2)/2$, and $\mathbf{x}' = (\mathbf{r}', t') = \mathbf{x}_1 - \mathbf{x}_2$, we can define the quasiclassical Green function by Fourier transforming $\check{G}(\mathbf{x}_1; \mathbf{x}_2)$ with respect to $\mathbf{x}'$ and integrating over $\xi_\mathbf{p} = \varepsilon_\mathbf{p} - E_F$ as

$$\check{g}(\mathbf{x}, \mathbf{n}, \epsilon) = \frac{i}{\pi} \int d\xi_\mathbf{p} \int d^4x' e^{i\epsilon t' - i\mathbf{p}\mathbf{r}'} \tau_3 \check{G}(\mathbf{x}_1; \mathbf{x}_2). \tag{3.6}$$

Here E_F is the Fermi energy, $\varepsilon_\mathbf{p}$ is the electron energy spectrum, and $\mathbf{n}$ is a unit vector labeling a location on the Fermi surface (for example, for a spherical Fermi surface it can be chosen as $\mathbf{n} = \mathbf{p}/|\mathbf{p}|$), and τ_3 is the third Pauli matrix. In this paper, we will denote the Pauli matrices in the Nambu space by τ_i, and the Pauli matrices in spin space by σ_i. The Keldysh space structure of the Green functions will be indicated explicitly when necessary.

The quasiclassical Green's function (3.6) satisfies the normalization condition

$$\check{g}\check{g} = 1, \tag{3.7}$$

which can be spelled out in terms of components in the Keldysh space as,

$$\hat{g}^{(R,A)}\hat{g}^{(R,A)} = 1, \tag{3.8}$$

$$\hat{g}^R\hat{g}^K + \hat{g}^K\hat{g}^A = 0. \tag{3.9}$$

The normalization condition Eq. (3.9) is satisfied for any Keldysh function of the form

$$\hat{g}^K = \hat{g}^R\hat{h} - \hat{h}\hat{g}^A. \tag{3.10}$$

The matrix $\hat{h}$ may be parameterized as[36]

$$\hat{h} = f_0\hat{\tau}_0 + f_1\hat{\tau}_3. \tag{3.11}$$

Here f_0 and f_1 are respectively the odd and even in ϵ parts of the distribution function (see Ref. [56] for an alternative treatment).

In this paper we only consider stationary situations. In this case the Green functions depend on the energy ϵ but not on the time t. If $k_F l \gg 1$ the Gorkov equation for the

Green function in Eq. (3.2) can be reduced to the quasi-classical Eilenberger equations for the Green functions defined in Eq. (3.6) [36]

$$i\mathbf{v}_F \cdot \boldsymbol{\nabla}\check{g} + \left[\epsilon\check{\tau}_3 - \check{\Delta}(\mathbf{n}) - \check{\Sigma}, \check{g}\right] = 0. \tag{3.12}$$

Here $\check{\Sigma}$ is the self energy associated with impurity scattering. In the Born approximation $\check{\Sigma} = -i\langle\check{g}\rangle/2\tau_e$, where $\langle\ldots\rangle$ denotes average over the solid angle in momentum space and τ_e is the elastic mean free time. The only difference of Eq. (3.12) from the conventional s-wave superconductor case is in the form Eq. (3.1) for the order parameter.

We neglect the electron-electron interactions in the normal metal. As a result, in our approximation the order parameter vanishes inside the normal metal. This yields the following equations for the retarded, advanced and Keldysh Green functions:

$$\begin{aligned} i\mathbf{v}_F \cdot \boldsymbol{\nabla}\hat{g}^{R,A} + \epsilon[\hat{\tau}_3, \hat{g}^{R,A}] &= [\hat{\Sigma}^{R,A}, \hat{g}^{R,A}], & (3.13)\\ i\mathbf{v}_F \cdot \boldsymbol{\nabla}\hat{g}^{K} + \epsilon[\tau_3, \hat{g}^{K}] &= \hat{\Sigma}^R\hat{g}^K + \hat{\Sigma}^K\hat{g}^A \\ &\quad -\hat{g}^R\hat{\Sigma}^K - \hat{g}^K\hat{\Sigma}^A. & (3.14) \end{aligned}$$

Multiplying Eq. (3.14) with τ_3 and τ_0 and taking the trace, and using the fact that $\mathrm{Tr}(\hat{g}^R - \hat{g}^A) = 0$, one obtains the following equations for f_1 and f_0

$$\begin{aligned} \mathrm{Tr}\left[\hat{\beta}\right]\mathbf{v}_F \cdot \boldsymbol{\nabla}f_1 &= -\frac{1}{2\tau_e}f_0\mathrm{Tr}\left(\langle\hat{\alpha}\rangle\hat{\alpha} - [\langle\hat{g}^R\rangle, \hat{g}^R] + [\langle\hat{g}^A\rangle, \hat{g}^A]\right) + \frac{1}{2\tau_e}\mathrm{Tr}\left[\langle\hat{\alpha}f_0\rangle\hat{\alpha}\right] \\ &- \frac{1}{2\tau_e}f_1\mathrm{Tr}\left(\langle\hat{\alpha}\rangle\hat{\beta} - [\langle\hat{g}^R\rangle, \hat{g}^R]\hat{\tau}_3 + \hat{\tau}_3[\langle\hat{g}^A\rangle, \hat{g}^A]\right) + \frac{1}{2\tau_e}\mathrm{Tr}\left[\langle\hat{\beta}f_1\rangle\hat{\alpha}\right], \quad (3.15) \\ \mathrm{Tr}\left[\hat{\beta}\right]\mathbf{v}_F \cdot \boldsymbol{\nabla}f_0 &= -\frac{1}{2\tau_e}f_0\mathrm{Tr}\left(\langle\hat{\tau}_3\hat{\beta}\hat{\tau}_3\rangle\hat{\alpha} - [\langle\hat{g}^R\rangle, \hat{g}^R]\hat{\tau}_3 + \hat{\tau}_3[\langle\hat{g}^A\rangle, \hat{g}^A]\right) + \frac{1}{2\tau_e}\mathrm{Tr}\left[\langle\hat{\alpha}f_0\rangle\hat{\tau}_3\hat{\beta}\hat{\tau}_3\right] \\ &- \frac{1}{2\tau_e}f_1\mathrm{Tr}\left(\langle\hat{g}^R\rangle\hat{\beta}\hat{\tau}_3 - \hat{\tau}_3\hat{\beta}\langle\hat{g}^A\rangle - [\langle\hat{g}^R\rangle, \hat{g}^R] + [\langle\hat{g}^A\rangle, \hat{g}^A]\right) \\ &+ \frac{1}{2\tau_e}\mathrm{Tr}\left[\langle\hat{\beta}f_1\rangle\hat{\tau}_3\hat{\beta}\hat{\tau}_3\right]. \quad (3.16) \end{aligned}$$

Here we defined $\hat{\alpha} = \hat{g}^R - \hat{g}^A$ and $\hat{\beta} = \hat{g}^R\hat{\tau}_3 - \hat{\tau}_3\hat{g}^A$.

The gauge-invariant potential and the electric current can be expressed in terms of quasiclassical Keldysh green functions as,

$$\begin{aligned} \Phi(\mathbf{r}) &= \frac{1}{4e}\int d\epsilon \int d^2\mathbf{n}\mathrm{Tr}\{\hat{g}^K(\mathbf{r}, \mathbf{n}, \epsilon)\} & (3.17)\\ J(\mathbf{r}) &= -\frac{e\nu_0}{4}\int d\epsilon \int d^2\mathbf{n}\mathbf{v}_F\mathrm{Tr}\{\hat{\tau}_3\hat{g}^K(\mathbf{r}, \mathbf{n}, \epsilon)\}. & (3.18) \end{aligned}$$

Here the integral over $\mathbf{n}$ denotes averaging over the Fermi surface, $d^2\mathbf{n} = d\Omega_{\mathbf{n}}/4\pi$.

We discuss the boundary conditions for the quasiclassical transport equations (3.12) - (3.16) in Sec. 3.2.1.

3.2.1 Boundary conditions for p-wave superconductor-normal metal interface

The p-wave superconductivity is destroyed by elastic scattering processes when $l < \xi_0$, where ξ_0 is the zero temperature coherence length in a clean superconductor. Therefore we consider the case where the p-wave superconductor is relatively clean and $l \gg \xi$. For the same reason the p-wave proximity effect is exponentially suppressed in the metal at distances larger than l from the boundary. On the other hand, in a spatially inhomogeneous system in the presence of spin-orbit interaction the p- and s- wave components of the anomalous Green functions are mixed. At low temperatures, the s-wave component induced by spin-orbit coupling extends into the metal to distances much larger than l, and determines the low temperature transport properties of the junction. Therefore spin-orbit coupling plays a crucial role in low temperature electron transport in normal metal–p-wave superconductor junctions.

Though our results have a general character, in this article we assume that a Rashba type spin orbit coupling is present only at the boundary. The corresponding potential energy at the boundary may be modeled by the form $V = (u_0\sigma_0 + u_1\hat{z} \times \mathbf{p}_\parallel \cdot \boldsymbol{\sigma})\delta(z)$, where $\mathbf{p}_\parallel$ is the component of the electron momentum parallel to the boundary, and $\hat{z}$ is the unit vector normal to the boundary. We assume that $u_1 \ll u_0$, and consider a disorder free boundary, so that $\mathbf{p}_\parallel$ is conserved.

The boundary conditions for quasiclassical Green functions in superconductors were obtained in Refs. [40, 41, 42]. In the case of a spin active boundary [42] they may be expressed in terms of the $\mathbf{p}_\parallel$-dependent scattering matrix of the insulating barrier. The latter relates the spinor amplitudes of the outgoing (ψ_o) and incident (ψ_i) electron waves,

$$\begin{pmatrix} \psi_o^S \\ \psi_o^N \end{pmatrix} = \begin{pmatrix} S_{11} & S_{12} \\ S_{21} & S_{22} \end{pmatrix} \begin{pmatrix} \psi_i^S \\ \psi_i^N \end{pmatrix}. \tag{3.19}$$

Here the superscripts N and S denote respectively the normal metal and the superconductor

side of the barrier. The presence of spin-orbit interaction at the boundary results in a spin-dependent transmission amplitude S_{12}, which may be written in the form

$$S_{12} = t_0 + t_s\gamma(\varphi_{\mathbf{n}}), \tag{3.20}$$

$$\gamma(\varphi_{\mathbf{n}}) = \cos\varphi_{\mathbf{n}}\sigma_y - \sin\varphi_{\mathbf{n}}\sigma_x. \tag{3.21}$$

Here we introduced the azimuthal angle $\varphi_{\mathbf{n}}$ as $\mathbf{p}_\parallel = |\mathbf{p}_\parallel|(\hat{x}\cos\varphi_{\mathbf{n}} + \hat{y}\sin\varphi_{\mathbf{n}})$. The spin-dependent and spin-independent transmission amplitudes t_s and t_0, are scalar functions of $|\mathbf{p}_\parallel|$. To lowest order in the transmission amplitude, the boundary condition for the quasiclassical Green functions may be written as [42]

$$\begin{aligned}\check{g}(\mathbf{r}^N, \mathbf{n}_o^N) &= -\frac{1}{2}\left[\check{S}_{21}\left(\check{g}(\mathbf{r}^S, \mathbf{n}_i^S) - 1\right)\check{S}_{21}^\dagger, \check{g}(\mathbf{r}^N, \mathbf{n}_o^N)\right] \\ &\quad + \check{S}_{22}\check{g}(\mathbf{r}^N, \mathbf{n}_i^N)\check{S}_{22}^{-1}, \end{aligned} \tag{3.22}$$

$$\begin{aligned}\check{g}(\mathbf{r}^S, \mathbf{n}_i^S) &= -\frac{1}{2}\left[\check{g}(\mathbf{r}^S, \mathbf{n}_i^S), \check{S}_{21}^\dagger\left(\check{g}(\mathbf{r}^N, \mathbf{n}_o^N) - 1\right)\check{S}_{21}\right] \\ &\quad + \check{S}_{11}^{-1}\check{g}(\mathbf{r}^S, \mathbf{n}_o^S)\check{S}_{11}. \end{aligned} \tag{3.23}$$

Here $\mathbf{n}_{i,o}^S$ and $\mathbf{n}_{i,o}^N$ are the unit vectors indicating positions on the Fermi surface in the superconductor (S) and the normal metal (N) for the incident (i) and outgoing (o) waves. By momentum conservation they correspond to the same $\mathbf{p}_\parallel$ and thus are characterized by the same azimuthal angle $\varphi_{\mathbf{n}}$. For simplicity we assume that Fermi surface in the superconductor to be a corrugated cylinder with the symmetry axis along $\hat{z}$, and that in the normal metal to be a sphere. The Fermi surface points corresponding to the incident and reflected waves are illustrated in Fig. 3.2. The coordinates $\mathbf{r}^N$ and $\mathbf{r}^S$ correspond respectively to the normal metal - and the superconductor- sides of the insulating boundary. For brevity the obvious ϵ dependence of Green functions has been dropped. Finally the matrices $\check{S}_{\alpha\beta}$ are defined following Ref. [42] as

$$\check{S}_{\alpha\beta} = S_{\alpha\beta}(\mathbf{p}_\parallel)\frac{1+\tau_3}{2} + S_{\beta\alpha}(-\mathbf{p}_\parallel)^T\frac{1-\tau_3}{2}, \tag{3.24}$$

where $S_{\alpha\beta}$ is defined in Eq. (3.20) and the superscript T denotes the matrix transposition in the spin space. At weak tunneling we may approximate $\check{S}_{11} \approx \check{S}_{22} \approx 1$, and

$$\check{S}_{12} = t_0\check{1} + t_s\check{\gamma}. \tag{3.25}$$

Here we introduced

$$\check{\gamma} = \begin{pmatrix} \hat{\gamma} & 0 \\ 0 & \hat{\gamma} \end{pmatrix}, \quad \hat{\gamma} = \begin{pmatrix} \gamma(\varphi_{\mathbf{n}}) & 0 \\ 0 & -\gamma(\varphi_{\mathbf{n}})^T \end{pmatrix}. \tag{3.26}$$

with $\gamma(\varphi_{\mathbf{n}})$ defined in Eq. (3.21).

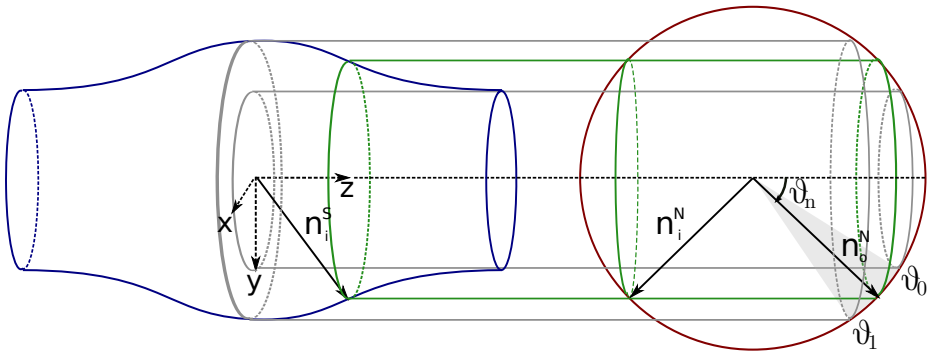

Figure 3.2: (color online) Fermi surface topologies of the superconductor (corrugated cylinder at left) and the normal metal (sphere at right). The vectors $\mathbf{n}_i$ and $\mathbf{n}_o$ correspond to respectively incident and outgoing waves. The superscripts N and S denote the superconductor and the normal metal sides of the insulating barrier. The vectors $\mathbf{n}^N$ and $\mathbf{n}^S$ correspond to the same parallel momentum, as shown by the green lines. The momentum domain where tunneling is possible is bounded by the angles ϑ_0 and ϑ_1. These angles define the integration limits in Eqs. (3.50) and (3.53).

For the purpose of studying electron transport at low temperatures, $T \ll \Delta$, we only need the Green functions with energies ϵ well below the gap Δ. The Green functions inside the superconductor are practically unaffected by tunneling. Therefore, the boundary condition for the normal metal Green function is given by Eq. (3.22), where the superconductor Green functions are replaced by their value in the bulk. Since latter do not depend on p_z we have $\check{g}(\mathbf{r}^S, \mathbf{n}_i^S) = \check{g}(\mathbf{r}^S, \mathbf{n}_o^S) \equiv \check{g}(\mathbf{r}^S, \mathbf{n}^S)$. It is useful to define symmetric and antisymmetric Green functions as [40, 41]

$$\check{g}_{s,a}(\mathbf{r}, \mathbf{n}) = \frac{1}{2}[\check{g}(\mathbf{r}, \mathbf{n}_i) \pm \check{g}(\mathbf{r}, \mathbf{n}_o)] \tag{3.27}$$

With this notation Eq. (3.22) may be written as follows:

$$\begin{aligned}\check{g}_a(\mathbf{r}^N,\mathbf{n}^N) &= -\frac{t_0^2}{4}\left[\check{g}(\mathbf{r}^S,\mathbf{n}^S),\check{g}_s(\mathbf{r}^N,\mathbf{n}^N)\right]\\ &\quad -\frac{t_0 t_s}{4}\left[\left\{\check{\gamma},\check{g}(\mathbf{r}^S,\mathbf{n}^S)\right\},\check{g}_s(\mathbf{r}^N,\mathbf{n}^N)\right]\\ &\quad +\frac{t_0 t_s}{2}\left[\check{\gamma},\check{g}_s(\mathbf{r}^N,\mathbf{n}^N)\right]. \end{aligned} \tag{3.28}$$

Here we for simplicity assume that due to weakness of spin-orbit coupling the electron tunneling amplitude with spin flip is smaller than that without, $t_s \ll t_0 \ll 1$. The first term in Eq. (3.28) arises from the spin-conserving tunneling and coincides with that in Ref. [40] at small transparency. This term dominates electron transport properties of the junction in the high temperature regime. The second term comes from the spin orbit coupling. Although it is smaller than the first one, it generates the s-wave component proximity effect in the normal metal and thus determines the electron transport at low temperatures. Finally, the last term is odd in the parallel momentum. Therefore it vanishes upon averaging over the Fermi surface and does not contribute to electron transport in the diffusive regime.

3.2.2 Kinetic scheme in the diffusive regime

In the low temperature regime, $T \ll v_F/l$, the proximity effect extends to distances of order $L_T = \sqrt{D/T} \gg l$ into the normal metal (here D is the electron diffusion constant). At such length scales the transport properties of the junction may be described in terms of the Usadel Green functions $\check{G}(\mathbf{r})$. The latter correspond to coincident coordinates of the electron operators in Eq. (3.2), $\mathbf{r} = \mathbf{r}'$, and may be expressed in terms of the Eilenberger Green functions (3.6) by averaging them over the Fermi surface

$$\check{G}(\mathbf{r}) = \int d^2\mathbf{n}\,\check{g}(\mathbf{r},\mathbf{n}), \quad d^2\mathbf{n} = \frac{1}{4\pi}\,d\cos\vartheta_{\mathbf{n}} d\varphi_{\mathbf{n}}. \tag{3.29}$$

where the polar and azimuthal angles $\vartheta_{\mathbf{n}}$ and $\varphi_{\mathbf{n}}$ characterize the unit vector $\mathbf{n} = (n_x, n_y, n_z) = (\sin\vartheta_{\mathbf{n}}\cos\varphi_{\mathbf{n}}, \sin\vartheta_{\mathbf{n}}\sin\varphi_{\mathbf{n}}, \cos\vartheta_{\mathbf{n}})$.

We neglect the spin-orbit interaction in the normal metal and assume that the electrons in the normal lead are not spin polarized. The triplet component of the anomalous Green function is exponentially suppressed at distances larger than l from the boundary with the

superconductor. The singlet component, on the other hand, survives even at distances much larger than l. Therefore it dominates the electron transport in the junction at low temperatures. Below we focus on the singlet component of the Usadel Green function, $\hat{G}(\mathbf{r})$, which is a 4×4 matrix in the Keldysh and Nambu space. Its various components $\alpha = R, A, K$ in the Keldysh space have the following form

$$\hat{G}^{\alpha}(\mathbf{r}) = \begin{pmatrix} G^{\alpha} & -iF^{\alpha} \\ i\tilde{F}^{\alpha} & -\tilde{G}^{\alpha} \end{pmatrix}. \tag{3.30}$$

The corresponding spin structure of the full 8×8 Green function in Eq. (3.29) is given by

$$\check{G}^{\alpha}(\mathbf{r}) = \begin{pmatrix} G^{\alpha}\sigma_0 & -iF^{\alpha}i\sigma_2 \\ i\tilde{F}^{\alpha}i\sigma_2 & -\tilde{G}^{\alpha}\sigma_0 \end{pmatrix}. \tag{3.31}$$

At length scales greater than l the singlet component of the Usadel Green function satisfies the differential equation

$$D\boldsymbol{\nabla} \cdot \left[\hat{G}(\mathbf{r})\boldsymbol{\nabla}\hat{G}(\mathbf{r})\right] + i\epsilon\left[\hat{\tau}_3, \hat{G}(\mathbf{r})\right] = 0. \tag{3.32}$$

Expanding in the Keldysh space, this equation gives

$$D\boldsymbol{\nabla} \cdot \left(\hat{G}^{(R,A)}\boldsymbol{\nabla}\hat{G}^{(R,A)}\right) + i\epsilon[\hat{\tau}_3, \hat{G}^{(R,A)}] = 0, \tag{3.33}$$

$$D\boldsymbol{\nabla} \cdot \left(\hat{G}^{R}\boldsymbol{\nabla}\hat{G}^{K} + \hat{G}^{K}\boldsymbol{\nabla}\hat{G}^{A}\right) + i\epsilon[\hat{\tau}_3, \hat{G}^{K}] = 0. \tag{3.34}$$

The first equation (3.33) is the Usadel equation, which describes the equilibrium properties of the system. The second equation (3.34) for Keldysh component describes the non-equilibrium properties. The Usadel Green function satisfies the normalization conditions (3.8) and (3.9). The condition (3.9) is satisfied by any matrix of the form (3.10). In the normal metal the matrix $\hat{h}$ may be expressed in terms of the symmetric and antisymmetric distribution functions f_0 and f_1 using Eq. (3.11). [36]

In a normal metal in contact with a single superconducting lead, Eq. (3.34) can be used to obtain following equations for distribution functions by using Eqs. (3.10) and (3.11):

$$\boldsymbol{\nabla} \cdot \left(\mathrm{Tr}\left[1 - \hat{G}^{R}(\mathbf{r})\hat{G}^{A}(\mathbf{r})\right]\boldsymbol{\nabla} f_0(\mathbf{r}, \epsilon)\right) = 0, \tag{3.35}$$

$$\boldsymbol{\nabla} \cdot \left(\mathrm{Tr}\left[1 - \tau_3\hat{G}^{R}(\mathbf{r})\tau_3\hat{G}^{A}(\mathbf{r})\right]\boldsymbol{\nabla} f_1(\mathbf{r}, \epsilon)\right) = 0. \tag{3.36}$$

The expressions for the density of states, electrochemical potential and current density in terms of the Usadel Green functions are

$$\nu(\mathbf{r},\epsilon) = \nu_0 \mathrm{Re}\left\{G^R(\mathbf{r},\epsilon)\right\}, \tag{3.37}$$

$$\Phi(\mathbf{r}) = \frac{1}{e\nu_0}\int d\epsilon \nu(\mathbf{r},\epsilon) f_1(\mathbf{r},\epsilon), \tag{3.38}$$

$$J(\mathbf{r}) = e\nu_0 D \int d\epsilon \Pi(\mathbf{r},\epsilon)\boldsymbol{\nabla} f_1(\mathbf{r},\epsilon). \tag{3.39}$$

Here $\Pi(\mathbf{r},\epsilon) = 1 + |G^R(\mathbf{r},\epsilon)|^2 + |F^R(\mathbf{r},\epsilon)|^2$, $\nu_0 = mp_F/\pi^2$ is the density of states of the normal metal in the absence of the proximity effect.

Using Eq. (3.8) one can write the retarded Usadel Green function in terms of the complex angles $\theta(\mathbf{r})$ and $\chi(\mathbf{r})$ as

$$\hat{G}^R(\mathbf{r}) = \begin{pmatrix} \cos\theta(\mathbf{r}) & -i\sin\theta(\mathbf{r})e^{i\chi(\mathbf{r})} \\ i\sin\theta(\mathbf{r})e^{-i\chi(\mathbf{r})} & -\cos\theta(\mathbf{r}) \end{pmatrix}. \tag{3.40}$$

The corresponding parametrization for advanced Green function can be obtained by using $\hat{G}^A(\mathbf{r}) = -\tau_3\left[\hat{G}^R(\mathbf{r})\right]^\dagger \tau_3$.

For the system of interest, where the normal metal is connected to a single superconductor the phase $\chi(\mathbf{r})$ is independent of coordinates and is set by the phase of the order parameter in the superconductor. In this case ($\boldsymbol{\nabla}\chi(\mathbf{r}) = 0$) the Usadel equation in (3.33) reduces to the following second order differential equation for the complex function $\theta(\mathbf{r})$:

$$\frac{D}{2}\boldsymbol{\nabla}^2\theta(\mathbf{r}) + i\epsilon\sin\theta(\mathbf{r}) = 0, \tag{3.41}$$

which is the well known sine-Gordon equation.

The equations for the distribution functions in (3.35) and (3.36) take the following forms in this parametrization:

$$D\boldsymbol{\nabla}\cdot\left(\cos^2\theta_R(\mathbf{r})\boldsymbol{\nabla} f_0(\mathbf{r})\right) = 0, \tag{3.42}$$

$$D\boldsymbol{\nabla}\cdot\left(\cosh^2\theta_I(\mathbf{r})\boldsymbol{\nabla} f_1(\mathbf{r})\right) = 0. \tag{3.43}$$

Here we introduced the real and imaginary parts of $\theta(\mathbf{r}) = \theta_R(\mathbf{r}) + i\theta_I(\mathbf{r})$.

Finally, using Eqs. (3.38), (3.39), and (3.40) we get the following expressions for the electric current and potential

$$J_n(\mathbf{r}) = eD\nu_0 \int d\epsilon \cosh^2\theta_I(\mathbf{r}) \boldsymbol{\nabla} f_1(\mathbf{r}) \tag{3.44}$$

$$\Phi(\mathbf{r}) = \frac{1}{e}\int d\epsilon \cos\theta_R(\mathbf{r}) \cosh\theta_I(\mathbf{r}) f_1(\mathbf{r}). \tag{3.45}$$

Below we will be interested only in linear in the external electric field effects, in which case $f_0 = \tanh(\epsilon/2T)$, has its equilibrium form.

The equations (3.33-3.34) or (3.41-3.43) must be supplemented with the boundary conditions. In Sec. 3.2.2 we obtain such conditions for a boundary between the normal metal and the p-wave superconductor in the geometry of our device.

Diffusive Boundary Conditions in the Vertical Geometry

The boundary conditions for the Usadel Green function $\hat{G}(\mathbf{r})$ may be found by solving the Eilenberger equations (3.12) with boundary conditions (3.28) at distances of the order of the mean free path l from the boundary. This can be done using the method of Ref. [41]. A key observation is that the Eilenberger equations (in which one may set $\epsilon \to 0$ for distances less than the mean free path from the boundary) conserve the matrix current normal to the boundary,

$$\check{j}(\mathbf{r}) = \int d^2\mathbf{n}\check{g}(\mathbf{r},\mathbf{n})\mathbf{v}_F \cdot \hat{z} = v_F \int' d^2\mathbf{n}\check{g}_a(\mathbf{r},\mathbf{n})\mathbf{n}\cdot\hat{z}. \tag{3.46}$$

The prime in the second expression indicates the fact that the integral must be taken over half the Fermi surface, $\mathbf{n}\cdot\hat{z} \geq 0$.

At weak tunneling the singlet component $\hat{j}$ of the matrix current at the boundary may be expressed in terms of the Usadel Green function $\hat{G}(\mathbf{r})$ as[41]

$$\hat{j}(\mathbf{r}^N) = D\hat{G}(\mathbf{r})\hat{z}\cdot\boldsymbol{\nabla}\hat{G}(\mathbf{r})|_{\mathbf{r}=\mathbf{r}^N}. \tag{3.47}$$

On the other hand, the matrix current may be evaluated by multiplying Eq. (3.28) with $v_F\mathbf{n}^N\cdot\hat{z}$ and integrating the result over half the Fermi surface, $\mathbf{n}^N\cdot\hat{z}\geq 0$. In doing so it is important to keep in mind that at weak tunneling the symmetric part of Green function in

the normal metal is independent of $\mathbf{n}^N$, $\check{g}_s(\mathbf{r}^N, \mathbf{n}^N) = \check{G}(\mathbf{r}^N)$, and that the superconductor Green function $\check{g}_s(\mathbf{r}^S, \mathbf{n}^S)$ may be replaced by its bulk value at $\epsilon = 0$. The latter is given by

$$\check{g}(\mathbf{n}) = -\begin{bmatrix} 0 & e^{i(\varphi_{\mathbf{n}}+\chi_0)}\mathbf{d}\cdot\boldsymbol{\sigma} i\sigma_2 \\ e^{-i(\varphi_{\mathbf{n}}+\chi_0)} i\sigma_2 \mathbf{d}^*\cdot\boldsymbol{\sigma} & 0 \end{bmatrix}. \tag{3.48}$$

Here we used Eq. (3.1). We consider unitary states, $\mathbf{d}\times\mathbf{d}^* = 0$, and parameterize the vector $\mathbf{d}$ by an overall phase χ_0 and the spherical angles $\vartheta_{\mathbf{d}}$, and $\varphi_{\mathbf{d}}$ as,

$$\mathbf{d}^T = e^{i\chi_0}(\sin\vartheta_{\mathbf{d}}\cos\varphi_{\mathbf{d}}, \sin\vartheta_{\mathbf{d}}\sin\varphi_{\mathbf{d}}, \cos\vartheta_{\mathbf{d}}). \tag{3.49}$$

It is easy to see that only the second term in the right hand side of Eq. (3.28) contributes to the matrix current. The contributions of the other two terms vanish upon the integration over $\mathbf{n}$ because both $\check{\gamma}$ and the superconductor Green function $\check{g}(\mathbf{r}^S, \mathbf{n}^S)$ depend on the azimuthal angle $\varphi_{\mathbf{n}}$ as $e^{\pm i\varphi_{\mathbf{n}}}$, see Eqs. (3.21), (3.26) and (3.48). We thus obtain

$$\check{j}(\mathbf{r}) = -\frac{v_F}{4}\int_{\vartheta_0}^{\vartheta_1}\frac{d\cos\vartheta_{\mathbf{n}}}{2} t_s t_0 \hat{z}\cdot\mathbf{n}\left[\check{\tilde{G}}(\mathbf{r}^S), \check{G}(\mathbf{r}^N).\right] \tag{3.50}$$

Here v_F is Fermi velocity in the normal metal, and the integration limits ϑ_0 and ϑ_1 define the domain where tunneling is possible. This domain corresponds to the projection of the corrugated cylindrical Fermi surface in the superconductor to the Fermi surface in the metal, see Fig. 3.2. Finally, $\check{\tilde{G}}(\mathbf{r}^S)$ is given by

$$\begin{aligned} \check{\tilde{G}}(\mathbf{r}^S) &\equiv \int \frac{d\varphi^S_{\mathbf{p}}}{2\pi}\left\{\check{g}(\mathbf{r}^S, \mathbf{n}^S_i), \check{\gamma}\right\} \\ &= \begin{bmatrix} 0 & e^{i(\varphi_{\mathbf{d}}+\chi_0)} i\sigma_2 \\ e^{-i(\varphi_{\mathbf{d}}+\chi_0)} i\sigma_2 & 0 \end{bmatrix}. \end{aligned} \tag{3.51}$$

Comparing Eqs. (3.47) and (3.50) we obtain the following boundary condition for the Usadel Green function,

$$D\check{G}(\mathbf{r})\partial_z\check{G}(\mathbf{r})|_{\mathbf{r}=\mathbf{r}^N} = t\left[\check{G}(\mathbf{r}^N), \check{\tilde{G}}(\mathbf{r}^S)\right], \tag{3.52}$$

where

$$t = \frac{1}{4}|\sin\vartheta_{\mathbf{d}}|\int_{\vartheta_0}^{\vartheta_1}\frac{d\cos\vartheta_{\mathbf{n}}}{2}(t_s t_0 v_F\cos\vartheta_{\mathbf{n}}). \tag{3.53}$$

Note that the boundary condition in Eq. (3.52) has the same structure as that for a boundary between an normal metal and an s-wave superconductor. The reason is that only

the s-wave component of the anomalous Green function survives in the normal metal at distances larger than l from the boundary. The difference however is that in our case the effective barrier transparency t in Eq. (3.53) depends on the spin-flip tunneling amplitude t_s, and on the vector $\mathbf{d}$ characterizing the spin orientation of the triplet order parameter. The phase of the effective s-wave anomalous Green function (3.51), $\chi_0 + \varphi_{\mathbf{d}}$, also depends on the orientation of the spin vector $\mathbf{d}$ in the xy-plane.

The aforementioned analogy enables one to treat the proximity effect in normal metal-p-wave superconductor systems in the diffusive regime as proximity effect in an effective s-wave superconductor problem, in which the phase of the s-wave order parameter and the barrier transparency depend on the spin orientation of the p-wave condensate.

It is convenient to recast the boundary condition Eq. (3.52) in terms of the parametrization in Eq. (3.40). In our setup, see Fig. 3.1, the phase $\chi(\mathbf{r})$ of the anomalous Usadel Green function (3.40) is uniform in space and equal to the phase of the effective s-wave order parameter, $\chi(\mathbf{r}) = \varphi_{\mathbf{n}} + \chi_0$. The boundary condition for the angle $\theta(\mathbf{r}^N)$ becomes

$$D\partial_z\theta(\mathbf{r})\big|_{\mathbf{r}=\mathbf{r}^N} = 2t\cos\left[\theta(\mathbf{r}^N)\right]. \tag{3.54}$$

The Keldysh component of the boundary condition in Eq. (3.52) gives the following boundary condition for the even part of the distribution function:

$$D\cosh^2\theta_I(\mathbf{r})\partial_z f_1(\mathbf{r})|_{\mathbf{r}=\mathbf{r}^N} \;=\; 2t\Gamma_\epsilon f_1(\mathbf{r}^N). \tag{3.55}$$

Here we assumed that $f_1(\mathbf{r}^S) = 0$ is zero inside superconductor and introduced the notation

$$\Gamma_\epsilon = \cosh\theta_I(\mathbf{r}^N)\sin\theta_R(\mathbf{r}^N). \tag{3.56}$$

The set of equations (3.41) and (3.43) along with the boundary conditions (3.54) and (3.55) gives a description of electron transport in diffusive metal–p-wave superconductor systems. Below we apply these equations to our device geometry.

3.3 Resistance of p-wave superconductor- normal metal junction

We consider the geometry in which the superconductor fills the $z < 0$ half space and the normal metal occupies the $z > 0$ half space, see Fig. 3.1. At weak tunneling the Green

function in the superconductor is practically unaffected by the presence of the tunneling barrier. On the other hand, the low energy properties of the normal metal are significantly affected by the proximity effect. The singlet Usadel Green function (3.30) in the normal metal is described by the set of equations (3.40), (3.41), (3.43) with the boundary conditions (3.54) and (3.55).

The solution of Eq. (3.41) satisfying the condition $\lim_{z\to\infty}\theta(z)=0$, has the form

$$\theta(\epsilon,z)=4\arctan\left[\exp\left(\beta_\epsilon+(i-1)\frac{z}{L_\epsilon}\right)\right]. \tag{3.57}$$

Here β_ϵ is an energy-dependent integration constant. Its value is determined from the boundary condition in Eq. (3.54), which gives

$$\cosh\beta_\epsilon-\frac{2}{\cosh\beta_\epsilon}=(1-i)\frac{L_t}{L_\epsilon} \tag{3.58}$$

where

$$L_t=\frac{D}{t},\quad L_\epsilon=\sqrt{\frac{D}{\epsilon}}. \tag{3.59}$$

The algebraic equation (3.58) has multiple solutions for the integration constant β_ϵ. The physical solution must satisfy the condition $\lim_{\epsilon\to 0}\theta(\epsilon,z=0+)=\pi/2$, which gives

$$e^{\beta_\epsilon}=\frac{\alpha+\sqrt{\alpha^2+8}}{2}-\frac{1}{2}\sqrt{(\alpha+\sqrt{\alpha^2+8})^2-4}, \tag{3.60}$$

where we introduced the notation $\alpha=(1-i)L_t/L_\epsilon$.

An important aspect of the solution Eq. (3.57) is that in the normal metal, at small values of ϵ and at small distances from the boundary, $\theta(z)\approx\pi/2$ which is the same as in the bulk of the superconductor. In particular, it means that at small energies the density of states in metal is strongly suppressed at distances smaller than L_ϵ. The full spatial dependence of the density of states $\nu(\epsilon,z)$ may be obtained by substituting the solution (3.57), (3.60) of the Usadel equation into Eqs. (3.37), and (3.40). In Fig. 3.3 we have plotted the result as a function of z/L_ϵ for different values of L_t/L_ϵ.

Note that the effective diffusion constant for the distribution function f_1 is determined by the imaginary part of θ, see Eq. (3.43). From the solution (3.57) it follows that the imaginary part θ_I is close to zero both at $z\gg L_\epsilon$ and $z\ll L_\epsilon$ and has a maximum at $z\sim L_\varepsilon$ whose value depends on L_ϵ/L_t. Therefore the effective diffusion coefficient in

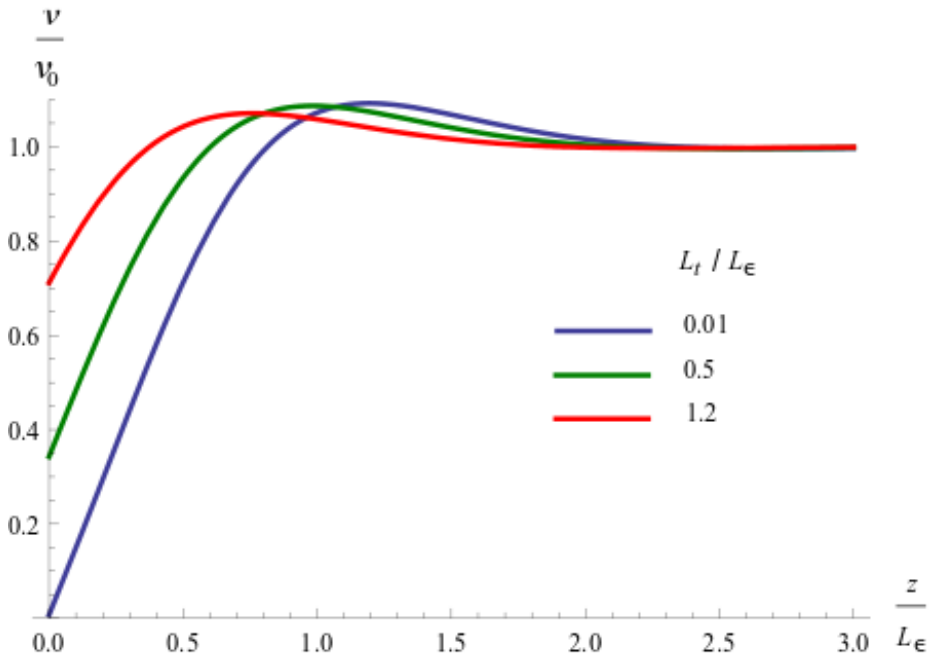

Figure 3.3: (color online) Density of states in the normal metal as a function of the distance from the superconductor-normal metal boundary for different temperatures: $L_t/L_\epsilon = 0.01$ (blue), $L_t/L_\epsilon = 0.5$ (green), and $L_t/L_\epsilon = 1.2$ (red).

Eq. (3.43) approaches its normal metal value at $z \gg L_\epsilon$ and $z \ll L_\epsilon$. In the intermediate region $z \sim L_\epsilon$ the diffusion coefficient exceeds the Drude value.

The differential equation (3.43) for the non-equilibrium part of the distribution function has the first integral, which has the meaning of the conserved partial current density at a given energy ϵ

$$J_\epsilon \equiv eD\nu_0 \cosh^2 \theta_I(z) \partial_z f_1(\epsilon, z). \tag{3.61}$$

The energy dependence of the partial current J_ϵ can be obtained by noticing that far away form the boundary the distribution function should have the form

$$f_1(\epsilon, z) = \frac{1}{\cosh^2 \frac{\epsilon}{2T}} \frac{eJ_0}{2T\sigma_D}(z - z_0), \tag{3.62}$$

where $\sigma_D = e^2\nu_0 D$ is the Drude conductivity of the normal metal, and we introduced the current density,

$$J_0 = \int_{-\infty}^{\infty} d\epsilon J_\epsilon. \tag{3.63}$$

Substituting Eq. (3.62) into Eq. (3.61) we obtain the following expression for the partial current

$$J_\epsilon = \frac{J_0}{4T}\frac{1}{\cosh^2\frac{\epsilon}{2T}}. \tag{3.64}$$

Using Eqs. (3.61) and (3.64) the solution of Eq. (3.43) which satisfies the boundary condition (3.55) and the asymptotic form (3.62) at large distances may be written in the form

$$f_1(\epsilon, z) = \frac{eJ_0}{2T\sigma_D \cosh^2\frac{\epsilon}{2T}}\left[\frac{L_t}{2\Gamma_\epsilon} + \int_0^z \frac{dz'}{\cosh^2\theta_I(\epsilon, z')}\right]. \tag{3.65}$$

Here $\theta_I(z')$ is given by Eqs. (3.57) and (3.60), and Γ_ϵ was defined in Eq. (3.56).

Substituting this result in Eq. (3.45) we get the following expression for the gauge invariant potential

$$\begin{aligned}\Phi(z) &= \frac{J_0}{\sigma_D}\int_0^\infty \frac{d\epsilon}{2T}\frac{\cos\theta_R(\epsilon, z)\cosh\theta_I(\epsilon, z)}{\cosh^2\frac{\epsilon}{2T}} \\ &\quad\times\left(\frac{L_t}{2\Gamma_\epsilon} + \int_0^z \frac{dz'}{\cosh^2\theta_I(\epsilon, z')}\right).\end{aligned} \tag{3.66}$$

In Fig. (3.4), we plotted the dependence of the gauge invariant potential on the dimensionless distance from the boundary, z/L_T, for different values of the dimensionless barrier transparency parameter, L_t/L_T.

One of the important features of transport through the junction is that at low temperatures the gauge invariant potential $\Phi(z)$ is significantly suppressed near the superconductor-normal metal boundary, and is a non-linear functions of z. In particular, the voltage drop across the insulator, $\Phi(z = 0)$, goes to zero in the low temperature limit.

Because of the nontrivial spatial distribution of the electric field in the junction its resistive properties may be characterized in different ways. One measure of the resistance can be defined in terms of the voltage drop across the insulating barrier. We define the resistance of the insulating boundary per unit area as

$$R_0 = \frac{\Phi(z = +0)}{J_0}. \tag{3.67}$$

Using Eq. (3.66) one can expression the boundary resistance R_0 per unit area in the form

$$R_0 = \frac{1}{e^2\nu_0 t}\frac{L_t}{L_T}A\left(\frac{L_t}{L_T}\right), \tag{3.68}$$

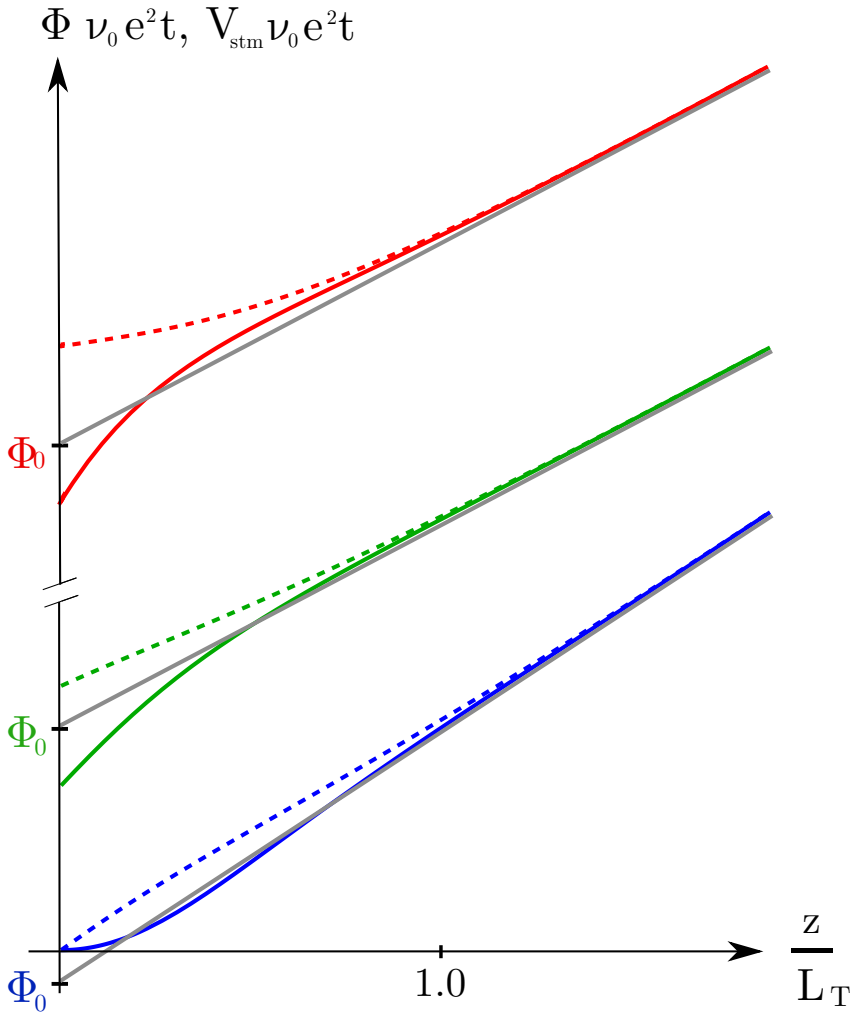

Figure 3.4: (color online) The spatial variation of the gauge-invariant potential Φ (solid lines) and the compensating voltage V_{stm} at the STM tip (dashed lines) on the dimensionless distance z/L_T from the boundary is plotted at different temperatures; $L_t/L_T = 0.01$ (blue), $L_t/L_T = 1$ (green) and $L_t/L_T = 5$ (red). The solid grey lines represent the large distance asymptotes of the gauge invariant potential. Their intercepts with the vertical axis for the three values of L_t/L_T are marked by Φ_0 in the corresponding color. The value of Φ_0 defines the junction resistance R_∞ in Eq. (3.70).

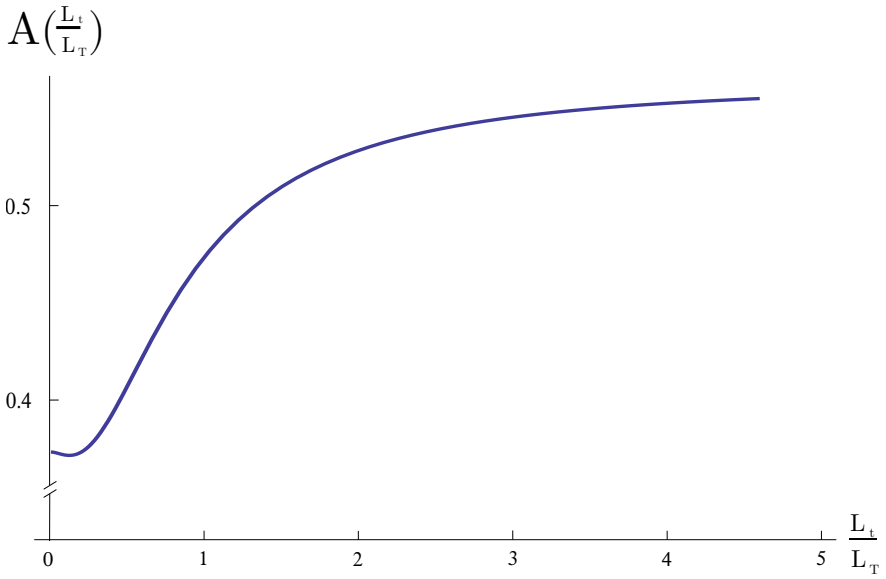

Figure 3.5: Plot of the function $A(L_t/L_T)$ in Eqs. (3.68), (3.69).

where the dimensionless function $A\left(L_t/L_T\right)$ is defined by the following integral

$$A\left(\frac{L_t}{L_T}\right) \;=\; \frac{L_T}{L_t}\int_0^\infty \frac{d\epsilon}{4T}\frac{\cot\theta_R(\epsilon,0)}{\cosh^2\frac{\epsilon}{2T}}. \tag{3.69}$$

This function is plotted in Fig. 3.5. In low and high temperature limits this expression tends to the following constants; $A(0)\approx 0.37$ and $A(\infty)\approx 0.53$. As a result in the high and low temperature regimes the boundary resistance $R_0\propto\sqrt{T}$.

Note that at low temperatures, $L_T \gg L_t$, the magnitude of the jump of $\Phi(z)$ at the insulator boundary approaches zero at $T\to 0$. This is very different from the resistance of the normal metal-insulator-normal metal junctions where in the presence of a current though the junction $R_{NIN}=1/e^2\nu_0\tilde{t}$, where $\tilde{t}\sim t_0^2$ is the transmission coefficient of the insulator.

Another measure of the junction resistance may be obtained by extrapolating the linear dependence of $\Phi(z)$ at large distances, $\Phi(z)=J_0 z/\sigma_D+\Phi_0$ to the location of the barrier, $z=0$. This is shown by grey solid lines in Fig. 3.4. The value of the intercept with the

vertical axis, Φ_0, defines the total resistance per unit area of the junction

$$R_\infty = \frac{\Phi_0}{J_0}. \tag{3.70}$$

Using Eq. (3.66) we obtain

$$R_\infty = \frac{1}{e^2 t\nu_0} B\left(\frac{L_t}{L_T}\right), \tag{3.71}$$

where the function $B(L_t/L_T)$ is given by the following integral

$$B = \int_0^\infty \frac{d\epsilon}{2T} \frac{1}{\cosh^2 \frac{\epsilon}{2T}} \left[\frac{1}{2\Gamma_\epsilon} - \int_0^\infty \frac{dz'}{L_t} \tanh^2 \theta_I(\epsilon, z')\right]. \tag{3.72}$$

The first term in the brackets is positive and represents the contribution of the insulating boundary. The second term is negative. It describes the reduction of the resistance of the normal metal due to the proximity effect.

The junction resistance R_∞ is plotted in Fig. (3.6) as a function of L_t/L_T. At relatively high temperatures $L_t/L_T \gg 1$, junction resistance R_∞ is dominated by the contribution from the insulating boundary (first term in Eq. (3.72)). In this case $B(L_t/L_T) \approx 0.53\, L_t/L_T$, in agreement with the discussion below Eq. (3.69). In the low temperature regime, $L_t \ll L_T$, the junction resistance is dominated by the change in the resistance of the normal metal due to the proximity effect (second term in Eq. (3.72) and becomes negative. In this case the junction resistance reduces to

$$R_\infty = -\frac{b}{e^2 t\nu_0} \frac{L_T}{L_t}, \tag{3.73}$$

where the constant b is given by

$$\begin{aligned} b &= \int_0^\infty \frac{d\lambda}{2} \frac{\lambda^{-1/2}}{\cosh^2 \frac{\lambda}{2}} \\ &\quad \times \int_0^\infty d\zeta \tanh^2 \left[4 \operatorname{Im} \arctan\left((\sqrt{2}-1)e^{(i-1)\zeta}\right)\right] \\ &\approx 0.39. \end{aligned} \tag{3.74}$$

3.3.1 Probing the spatial distribution of the gauge-invariant potential $\Phi(\mathbf{r})$

Let us now discuss the possibility of experimental observation of the suppression of $\Phi(x)$ near the junction's boundary by using a scanning tunneling probe. We consider the setup illustrated in Fig. 3.1.

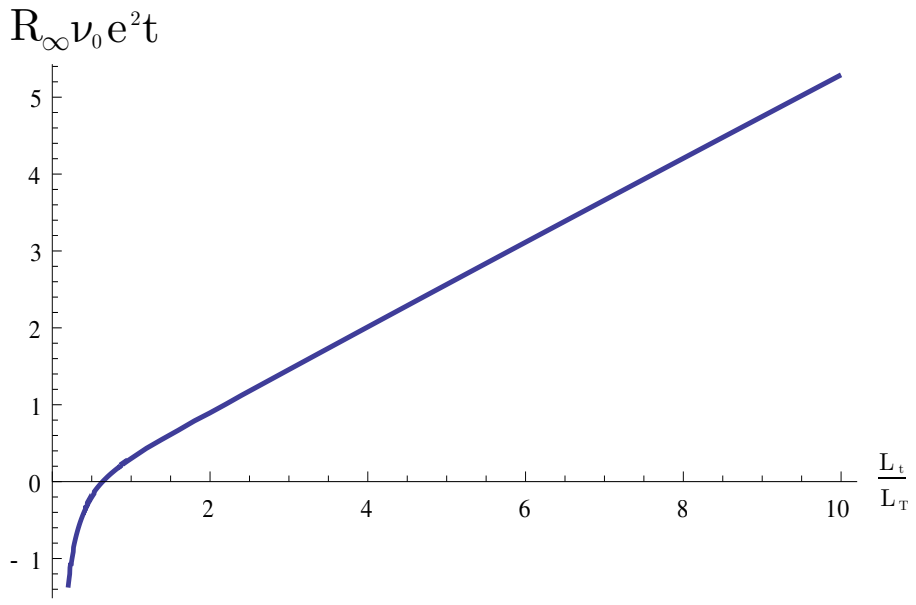

Figure 3.6: The junction resistance R_∞ per unit area (in units of $1/e^2\nu_0 t$) is a plotted as a function of L_t/L_T.

The electron transport between the STM tip and the metal can be described with the aid of the tunneling Hamiltonian

$$H_T = \sum_{\mathbf{kp}} \left[t_{\mathbf{kp}} c^\dagger_{\mathbf{k}} c_{\mathbf{p}} + t^*_{\mathbf{kp}} c^\dagger_{\mathbf{p}} c_{\mathbf{k}} \right]. \tag{3.75}$$

Here $c^\dagger$ is an electron creation operator, and $\mathbf{k}$ labels the states in the STM tip and $\mathbf{p}$ labels the states in the wire. In the tunneling approximation the STM current can be written in the form

$$\begin{aligned} I_{stm}(z) &= \frac{g_n}{2e} \int_{-\infty}^{\infty} d\epsilon \cos\theta_R(\epsilon, z) \cosh\theta_I(\epsilon, z) \\ &\quad \times \left[f_1^{stm}(\epsilon) - f_1(\epsilon, z) \right], \end{aligned} \tag{3.76}$$

where g_n is the conductance of the tunneling contact in the normal state. The nonequilibrium distribution function in the STM is given by $f_1^{stm}(\epsilon) = eV_{stm}/2T\cosh^2(\epsilon/2T)$, where V_{stm} is the STM voltage measured relative to that in the superconductor.

Using Eq. (3.45) we can rewrite Eq. (3.76) in the form

$$I_{stm}(z) = g_n \Phi(z) - g_t(T, z) V_{stm}, \tag{3.77}$$

where

$$g_t(T,z) = g_n \int_0^\infty \frac{d\epsilon}{2T} \frac{\cos\theta_R(\epsilon,z)\cosh\theta_I(\epsilon,z)}{\cosh^2\frac{\epsilon}{2T}} \tag{3.78}$$

is the conductance of the tunneling contact.

In the case where the voltage V_{stm} at the tip vanishes the value of the tunneling current through the STM contact is proportional to $\Phi(z)$,

$$I_{stm}(z) = g_n \Phi(z). \tag{3.79}$$

In particular, $I_{stm}(z)$ is significantly suppressed near the superconductor-normal metal boundary, reflecting corresponding suppression of $\Phi(x)$.

On the other hand, if $I_{stm} = 0$, we get

$$V_{stm}(z) = \frac{g_n}{g_t(T,z)}\,\Phi(z), \tag{3.80}$$

where $\Phi(z)$ is given by Eq. (3.66). The graph of $V_{stm}(z)$ is plotted in Fig. 3.4 by dashed lines for several temperatures. It is interesting to note that, in contrast to the gauge invariant potential, Eq. (3.79), the compensating STM voltage in Eq. (3.80) does not exhibit the aforementioned suppression near the boundary at low temperatures, $L_T \gg L_t$. The slope $dV_{stm}(z)/dz$ remains practically the same as in the normal metal in the absence of superconductor, both at $z \ll L_T$ and at $z \gg L_T$. The reason is that the conductance of the tunneling barrier between the STM and the metal, $g_t(T,z)$, reflects the suppression of the single particle density of states in the metal, as described by Eq. (3.78). This nearly cancels the suppression of $\Phi(z)$ in Eq. (3.80).

3.4 Conclusions

We show that the low temperature resistance of the p-wave superconductor-diffusive normal metal junctions is controlled by the spin-orbit interaction. As a result the junction resistance, tunneling density of states in the metal and other transport properties of the device exhibit a strong dependence on the angle between the vector **d** characterizing the spin part of the superconducting wave function, and the normal to the surface of the junction. In particular, the s-wave component of the proximity effect in metal vanishes when **d** is parallel to the c-axis.

The absence of the corresponding dependence of the Knight shift on the angle between **d** and the c-axis in Sr_2RuO_4 crystals is one of the problems in the interpretation of Sr_2RuO_4 as a conventional p-wave superconductor. This fact was attributed to weakness of the spin-orbit interaction in Sr_2RuO_4.[55] We would like to point out that the resistance of the junction should be strongly dependent on the angle between **d** and **z** even in the case of weak spin-orbit interaction. Therefore the measurement of this effect could clarify the situation.

Another consequence of the sensitivity of the proximity effect to the orientation of the condensate spin is that a current passing across such a junction leads to spin accumulation inside the p-wave superconductor (although inside the proximity region no spin accumulation occurs).

We also would like to mention that the boundary conditions Eq. (3.52) can be used to describe the Josephson effect in junctions consisting of two p-wave superconductors separated by a diffusive normal metal. The structure of boundary conditions (3.52) is similar to those of for s-wave superconductor-normal metal junction. Therefore the supercurrent for the p-wave case may be obtained from the conventional formulas for the s-wave case if we substitute the phase difference in the s-wave case with $\phi_{\mathbf{d}} + \chi_0$, see Eqs. (3.51) and (3.49), and the transmission coefficient with t.

An important consequence of the proximity effect near the superconductor-normal metal boundary is the suppression of the Hall effect in the metal near the superconducting boundary. Qualitatively, this suppression is related to the fact that, due to proximity effect, at low energies the quasiparticle wave functions in metal are a coherent superposition of electron and hole wave functions, and the effective charge of the quasiparticles approaches zero at $\epsilon \to 0$. The presented above scheme of calculation of the electronic transport was derived in zeroth order in $\omega_c\tau$, where ω_c is the cyclotron frequency and τ is the elastic mean free time. In this approximation the electron wave functions near the Fermi surface are electron-hole symmetric, which yields a vanishing Hall effect. To describe Hall effect one has to add to the expression for the current a term linear in $\omega_c\tau$,[57]

$$\mathbf{J}_H \propto \omega_c\tau \mathbf{b} \times \int d\epsilon \cos\theta_R \cosh^3\theta_I \boldsymbol{\nabla} f_1 \tag{3.81}$$

here ω_c is the cyclotron frequency, and $\mathbf{b}$ is the unit vector in the direction of the magnetic field. Since the magnitude of the proximity effect is controlled by t, which is proportional to $\sin\vartheta_{\mathbf{d}}$, the Hall conductance is expected to have a strong dependence on the orientation of the order parameter, $\mathbf{d}$. Since the latter may be oriented by the external magnetic field, both the magnetoresistance of the junction and the Hall resistance are expected to be strongly anisotropic with respect to orientation of the magnetic field.

Finally, we note that our results hold for more general realizations of $p_x + ip_y$ order parameter in superconductors with complicated topology of the Fermi surface, such as the one proposed in Ref. [25].

Chapter 4

THEORY OF DISORDERED UNCONVENTIONAL SUPERCONDUCTORS

Some parts of this chapter are based on A. Keles, A.V. Andreev, S. A. Kivelson and B.Z. Spivak "Theory of unconventional superconductors" arXiv:1405.7090 (2014).

In contrast to conventional s-wave superconductivity, unconventional (e.g. p or d-wave) superconductivity is strongly suppressed even by relatively weak disorder. Upon approaching the superconductor-metal transition, the order parameter amplitude becomes increasingly inhomogeneous leading to effective granularity and a phase ordering transition described by the Mattis model of spin glasses. One consequence of this is that at low enough temperatures, between the clean unconventional superconducting and the diffusive metallic phases, there is necessarily an intermediate superconducting phase which exhibits s-wave symmetry on macroscopic scales.

4.1 Disorder in s-wave superconductors

Let us first consider the effect of non-magnetic impurities in conventional s-wave superconductors. Our starting point is self-consistency equation given in Eq. 2.11. In the case of s-wave pairing, interaction term can be taken as constant as in the usual BCS theory. Since disorder is random by its nature, one has to perform ensemble averaging over the realization of impurities which is the essence of diagrammatic technique. For performing this program, it is convenient to define a vertex correction. Summing up the terms to infinite order one can obtain following Dyson equation for the vertex correction:

$$\Gamma(\mathbf{p},\omega_n) = \Delta + \frac{n_i}{(2\pi)^3}\int \mathrm{d}^3\mathbf{p}'|U_{\mathbf{p}\mathbf{p}'}|^2 G^{(0)}(\mathbf{p}',\omega_n)G^{(0)}(-\mathbf{p}',-\omega_n)\Gamma(\mathbf{p}',\omega_n) \qquad (4.1)$$

where we have used normal state Green functions as given in Eq. 2.15 above and $|U_{\mathbf{p}\mathbf{p}'}|$ is the disorder potential. With the definition in Eq. 4.1, self consistency equation can be

written as

$$\Delta = gT \sum_{\omega_n} \int \frac{\mathrm{d}^3\mathbf{p}}{(2\pi)^3} G^{(0)}(\mathbf{p}, \omega_n) G^{(0)}(-\mathbf{p}, -\omega_n) \Gamma(\mathbf{p}, \omega_n) \tag{4.2}$$

where g is the constant interaction term in the BCS approximation. The integrals appearing in Eq. 4.1 and 4.2 are calculated by following prescription:

$$\int \frac{\mathrm{d}^3\mathbf{p}}{(2\pi)^3} = \nu_0 \int_{-\infty}^{\infty} \mathrm{d}\xi \int \frac{\mathrm{d}\Omega_{\mathbf{p}}}{4\pi} \tag{4.3}$$

where ν_0 is the density of states at the Fermi level and $\Omega_{\mathbf{p}}$ is the solid angle at the Fermi surface. This enables contour evaluation of the remaining integrals in the complex-ξ plane which are straightforward. From the computation of the expression in Eq. 4.1 one can obtain

$$\Gamma(\mathbf{p}, \omega_n) = \Delta_0 \left(1 + \frac{1}{\tau_e} \frac{\mathrm{sgn}\omega_n}{\omega_n} \right) \tag{4.4}$$

which is momentum independent and we defined elastic scattering time in Born approximation as

$$\frac{1}{\tau_e} = n_i \int \frac{\mathrm{d}\Omega_{\mathbf{p}}}{4\pi} |U_{\mathbf{p}\mathbf{p}'}|^2 \tag{4.5}$$

and assumed that scattering potential depends only on the direction of the momentum. Here n_i is the concentration of impurities. Finally, substituting this result in Eq. 4.2 and performing the integrations in a similar way it is easy to obtain the following equation for the transition temperature:

$$1 = V_0 \nu_0 2\pi T \sum_{\omega_n > 0} \frac{1}{\omega_n} \tag{4.6}$$

which is independent of impurity concentration and same as in the clean case. Note that this result is correct for small values of impurity levels but cannot be continued to strong impurity regime which obviously gives nonsense.

4.2 Suppression of unconventional superconductivity with disorder

Let us consider the change of the transition temperature in the case of unconventional superconductors. Here we explicitly take a momentum dependent order parameter and consistently momentum dependent attractive potential for pairing in non-zero angular momentum states.

To be more specific, we consider the p-wave pairing as in the case of superfluid ^{3}He or two dimensional analog Sr_2RuO_4. Linearized self-consistency equation for the pairing amplitude in the Gor'kov formalism is given by

$$\Delta_{\mu\nu}(\mathbf{k},\mathbf{q}) = T\sum_n \sum_{\mathbf{k}'\mathbf{k}''\mathbf{q}'} V_{\mathbf{k}\mathbf{k}'} G_w(\mathbf{k}'+\frac{\mathbf{q}}{2},\mathbf{k}''+\frac{\mathbf{q}'}{2}) G_{-w}(-\mathbf{k}'+\frac{\mathbf{q}}{2},-\mathbf{k}''+\frac{\mathbf{q}'}{2}) \Delta_{\mu\nu}(\mathbf{k}'',\mathbf{q}') \quad (4.7)$$

Corresponding potential between the Cooper pairs is assumed to be in the p-wave channel which is given as

$$V_{\mathbf{k}\mathbf{k}'} = -3g\frac{\mathbf{k}\cdot\mathbf{k}'}{k_F^2}. \quad (4.8)$$

The order parameter for a p-wave superconductor can be parametrized in the following way considering a triplet spin part,

$$\Delta_{\mu\nu}(\mathbf{k},\mathbf{q}) = (\sigma_\alpha i\sigma_2)_{\mu\nu} A_{\alpha i}(\mathbf{q}) k_i. \quad (4.9)$$

Inserting this expression into self consistency equation and canceling the k_i and $(\sigma_\alpha i\sigma_2)_{\mu\nu}$ from both sides gives the following expression

$$A_{\alpha i}(\mathbf{q}) = 3gT\sum_n \sum_{\mathbf{k}'\mathbf{k}''\mathbf{q}'} \frac{k_i' k_j''}{k_F^2} G_w(\mathbf{k}'+\frac{\mathbf{q}}{2},\mathbf{k}''+\frac{\mathbf{q}'}{2}) G_{-w}(-\mathbf{k}'+\frac{\mathbf{q}}{2},-\mathbf{k}''+\frac{\mathbf{q}'}{2}) A_{\alpha j}(\mathbf{q}') \quad (4.10)$$

For simlicity, lets take $\mathbf{q} = \mathbf{q}'$ in Eq. 4.10

$$A_{\alpha i}(\mathbf{q}) = 3gT\sum_n \sum_{\mathbf{k}'\mathbf{k}''} \frac{k_i'}{k_F} G_w(\mathbf{k}'+\frac{\mathbf{q}}{2},\mathbf{k}''+\frac{\mathbf{q}}{2}) G_{-w}(-\mathbf{k}'+\frac{\mathbf{q}}{2},-\mathbf{k}''+\frac{\mathbf{q}}{2}) \frac{k_j''}{k_F} A_{\alpha j}(\mathbf{q}) \quad (4.11)$$

The transition temperature is obtained from the largest eigenvalue of this linear integral equation. It can be shown from this expression that highest transition temperature is given for $\mathbf{q} = 0$ and the remaining integral equation will have a similar form as in the s-wave case with one very important difference. In the case of p-wave, we have vector vertices which means any diagram with an impurity line gives zero contribution due to angular integrations so that vertex corrections will drop out of the equations. The resulting Green functions in the above integral should be separately averaged which gives imaginary parts to the denominators and the resulting integral can be calculated considering the same equation for zero disorder giving the following equation

$$1 = g\nu_0 2\pi T \sum_{\omega_n>0} \frac{1}{\omega_n} + g\nu_0 2\pi T \sum_{\omega_n>0} \frac{1}{\omega_n + 1/2\tau} - \frac{1}{\omega_n} \quad (4.12)$$

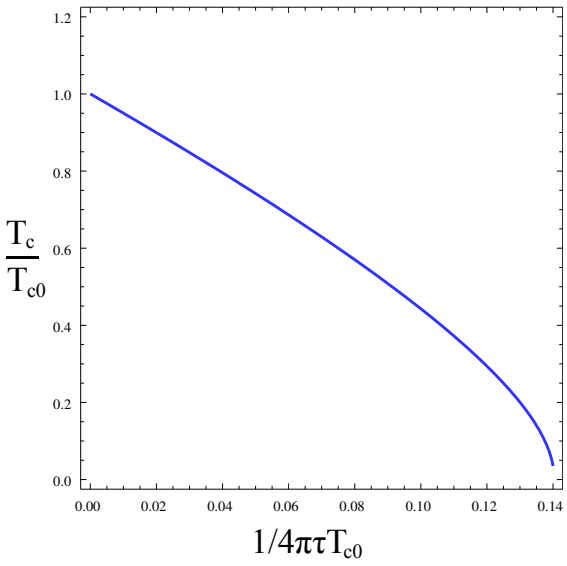

Figure 4.1: Change of transition temperature as a function of increasing disorder

Using the definition of digamma function ψ, the following form can be obtained for the transition temperature

$$\ln \frac{T_{c0}}{T_c} = \psi(\frac{1}{2} + \frac{1}{4\pi\tau_e T_c}) - \psi(\frac{1}{2}) \tag{4.13}$$

where the transition temperature in the clean case is given by

$$T_{c0} = \frac{2\gamma}{\pi}\omega_D e^{-1/\nu_0 g} \tag{4.14}$$

The nonlinear equation given in Eq. 4.13 is plotted in Fig. 4.1 which shows suppression of transition temperature with increasing disorder

One can substitute the order parameter for d-wave superconductor given as

$$\Delta_{\mu\nu}(\mathbf{k}, \mathbf{q}) = i(\sigma_2)_{\mu\nu} A^d(\mathbf{q})(k_x^2 - k_y^2) \tag{4.15}$$

in the linearized self-consistency equation to obtain similar conclusion for the effect of impurities in high temperature superconductors.

4.3 Theory of disordered unconventional superconductors

Generally, the superconducting order parameter depends on two coordinates and two spin indices, $\Delta_{\alpha\beta}(\mathbf{r}, \mathbf{r}')$. A classification of possible superconducting phases in crystalline ma-

terials was given in Refs. [58] and [59]. The majority of crystalline superconductors with low transition temperature have a singlet order parameter with an s-wave orbital symmetry that does not change under the rotation of the coordinates. In the simplest case, it can be described by single coordinate, $\Delta_{\alpha\beta}(\mathbf{r},\mathbf{r}') = i(\hat{\sigma}_2)_{\alpha\beta}\delta(\mathbf{r}-\mathbf{r}')\Delta^{(s)}(\mathbf{r})$ where $\hat{\sigma}_2$ is second Pauli matrix in spin space, $\Delta^{(s)}(\mathbf{r})$ is a complex valued function and superscript s indicates that is has s-wave symmetry. However, over the last decades a number of superconductors have been discovered in which the order parameter transforms according to a non-trivial representation of the point group of underlying crystal. Although such superconductors are quite common by now, following the terminology of Ref. [7], we refer to them as being unconventional.

Important examples include the high temperature cuprate superconductors which have a singlet d-wave symmetry[59, 60]: $\Delta_{\alpha\beta}(\mathbf{r},\mathbf{r}') = i(\hat{\sigma}_2)_{\alpha\beta}\Delta^{(d)}(\mathbf{r}-\mathbf{r}')$ where $\Delta^{(d)}(\mathbf{r}-\mathbf{r}')$ changes sign under coordinate rotation by $\pi/2$. The best known example of a p-wave superfluid is superfluid ^{3}He. One of the leading candidates for p-wave pairing in electronic systems is Sr_2RuO_4.[1] There are numerous pieces of experimental evidence that the superconducting state of Sr_2RuO_4 has odd parity, breaks time reversal symmetry and is spin triplet.[49, 50, 21, 51, 1, 20] An order parameter consistent with these experiments is given by the chiral p-wave state [17] which has the form $\Delta_{\alpha\beta}(\mathbf{p}) \sim p_x \pm ip_y$ where $\Delta_{\alpha\beta}(\mathbf{p})$ is the Fourier transform of $\Delta_{\alpha\beta}(\mathbf{r}-\mathbf{r}')$. Anderson's theorem accounts for the fact that superconductivity in s-wave superconductors is destroyed only when the disorder is so strong that $p_F l \sim 1$, where p_F is the Fermi momentum and l is the electronic elastic mean free path. However, since in the unconventional superconductors $\Delta_{\alpha\beta}(\mathbf{p})$ depends on the direction of the relative momentum $\mathbf{p}$ of the electrons in the Cooper pair, they are much more sensitive to disorder; even at zero temperature, unconventional superconductivity is destroyed when l is comparable to the zero temperature coherence length in the pure superconductor, $l \sim \xi_0 \gg 1/p_F$. The fate of unconventional superconductivity subject to increasing disorder depends on the sign of the interaction constant in the s-wave channel. It is straightforward to see that if the interaction in the s-wave channel is attractive, but weaker than the attraction in an unconventional channel, then as a function of increasing disorder, there will first be a transition from the unconventional to an s-wave phase when $l \sim \xi_0$, followed by a transition

to a non-superconducting phase when $l \sim p_F^{-1}$. Here ξ_0 is the correlation length of the unconventional superconductor in the limit of vanishing disorder.

In this article we consider the more interesting and realistic case, in which the interaction in the s-channel is repulsive. In this case, we show that there is necessarily a range of disorder strength in which, although locally the pairing remains unconventional, the system has a global s-wave symmetry with respect to any macroscopic superconducting interference experiments. Therefore there must be at least two phase transitions as a function of increasing disorder: a d-wave (or p-wave) to s-wave, followed by an s-wave to normal metal transition. Qualitatively the phase diagram of disordered unconventional superconductors is shown in Fig. 4.3 (An incomplete derivation of these results – only for the d-wave case – was obtained in Refs. [61] and [62].)

The existence of the intermediate s-wave superconducting phase between the unconventional superconductor and the normal metal (and of the corresponding s-wave to unconventional superconductor transition) can be understood at a mean field level which neglects both classical and quantum fluctuations of the order parameter. The electron mean free path is an average characteristic of disorder. Let us introduce a local value of the mean free path $\bar{l}(\mathbf{r})$ averaged over regions with a size of order ξ_0. When the disorder is sufficiently strong such that, on average, $\bar{l} < \xi_0$, the superconducting order parameter will only be large in the rare regions which satisfies $\bar{l}(\mathbf{r}) > \xi_0$. In this case, the system can be visualized as a matrix of superconducting islands that are coupled through Josephson links in a non-superconducting metal. (The superconductivity inside an island can be enhanced if the pairing interaction is stronger than average, *i.e.* if the local value of ξ_0 is anomalously small.) At sufficiently large values of disorder the distance between the islands is larger than both their size and the mean free path.

4.4 Mattis model description of disordered unconventional superconductors

Below we show that in the vicinity of superconductor-normal metal transition the superconducting phase may be described by the Mattis model.

4.4.1 An isolated superconducting island

To begin with, we consider the mean-field description of an isolated superconducting island. Order parameter in an individual island is written as $\hat{\Delta}_a(\mathbf{r}, \mathbf{r}')$ where hat indicates the two by two matrix structure in spin space and we label the individual islands with Latin indices a, b, ... Generally, neither the shape of the island nor the texture of the pairing tendencies within it have any particular symmetry, so the resulting gap function $\hat{\Delta}_a(\mathbf{r}, \mathbf{r}')$ mixes the symmetries of different bulk phases. Since there is no translational symmetry, it is convenient to define $\hat{\Delta}_a(\tilde{\mathbf{r}}, \mathbf{p})$ as the Fourier transform of $\hat{\Delta}_a(\mathbf{r}, \mathbf{r}')$ with respect to relative coordinates $\mathbf{r} - \mathbf{r}'$ and use a new variable $\tilde{\mathbf{r}} = (\mathbf{r} + \mathbf{r}')/2$ as the center of mass coordinate (Since all of the coordinates to appear from now on are the center of mass coordinates, we drop tilde in our notation). In the absence of spin-orbit coupling, a sharp distinction exists between spin-0 (singlet) and spin-1 (triplet) pairing, although even that distinction is entirely lost in the presence of spin-orbit coupling. The most general form of the gap function (with a phase convention which we will specify later) expressed as a second rank spinor in terms of Pauli matrices is

$$\hat{\Delta}_a(\mathbf{r}, \mathbf{p}) = e^{i\phi_a}\ i\hat{\sigma}_2 \left(\Delta_a \hat{1} + \mathbf{\Delta}_a \cdot \hat{\boldsymbol{\sigma}}\right). \tag{4.16}$$

where we have left implicit the $\mathbf{r}$ and $\mathbf{p}$ dependence of the scalar Δ_a and vector $\mathbf{\Delta}_a$ quantities that represent the singlet and triplet components of the order parameter.

The energy of a single grain is independent of the overall phase of the order parameter ϕ_a. In the absence of spin-orbit interaction it is also independent of the direction $\mathbf{\Delta}_a$. An additional discrete degeneracy may be associated with time-reversal invariance of the problem. The latter implies that the state described by a time-reversed order parameter

$$\hat{\bar{\Delta}}_a(\mathbf{r}, \mathbf{p}) \equiv -i\hat{\sigma}_2[\hat{\Delta}_a(\mathbf{r}, -\mathbf{p})]^* i\hat{\sigma}_2 \tag{4.17}$$

leads to the same energy in the grain. In the absence of spontaneous breaking of time reversal symmetry the time reversal operation leads to the same physical state $\hat{\bar{\Delta}}_a = \hat{\Delta}_a$, otherwise the time-reversed state is physically different.

It is important to note that generally the time reversal symmetry is violated in droplets of unconventional superconductors of a random shape. This occurs even in the case where

a bulk phase of unconventional superconductor is time reversal invariant, such as d-wave superconductors or p_x, p_y phases realized in strained Sr_2RuO_4 [63]. For example, d-wave superconducting droplets of a random shape embedded into a bulk metal with a certain probability can form geometry of a corner SQUID experiment [60] where two sides of a droplet with different signs of the order parameter are connected by a metallic Josephson link with negative critical current. A current will flow in the ground state of the system provided the critical current of the "negative link" is larger that the critical current in a bulk.

We will characterize the degeneracy with respect to time reversal by a pseudo-spin index $\xi = \pm 1$. In this case it is convenient to introduce a pseudospin ξ in each grain that will distinguish the two time-reversed states,

$$\hat{\Delta}_a^{\xi}(\mathbf{r}, \mathbf{p}) = \begin{cases} \hat{\Delta}_a(\mathbf{r}, \mathbf{p}), & \xi = +1 \\ \hat{\bar{\Delta}}_a(\mathbf{r}, \mathbf{p}), & \xi = -1 \end{cases} \tag{4.18}$$

and write the general expression for the order parameter in each grain as

$$e^{i\phi_a} \hat{\Delta}_a^{\xi}(\mathbf{r}, \mathbf{p}). \tag{4.19}$$

where we explicitly separate the U(1) phase of the order parameter.

4.4.2 Josephson coupling between islands

Electrons propagating in the non-superconducting metals experience Andreev reflection [64] from the superconducting islands. This induces Josephson coupling between the islands. At large separations between the islands the Josephson coupling will not alter the spatial dependence of the order parameter in the grain $\hat{\Delta}_a^{\xi}(\mathbf{r}, \mathbf{p})$. Therefore the low energy Hamiltonian of the system may be expressed in terms of the phases ϕ_a only. The energy of this coupling can be expressed in the form

$$E_J = -\frac{1}{2} \sum_{a \neq b} J_{ab}^{\xi\xi'} \cos(\phi_a - \phi_b + \theta_{ab}^{\xi\xi'}) \tag{4.20}$$

Here $J_{ab}^{\xi\xi'} > 0$ is the Josephson coupling energy between the islands a and b, and $\theta_{ab}^{\xi\xi'}$ is the phase which is determined by the spatial dependence of the complex order parameter in the grains, $\hat{\Delta}_a^{\xi}(\mathbf{r}, \mathbf{p})$.

Our goal is to show that if the distance between the islands is larger than their size then the link phases may be written as

$$\theta_{ab}^{\xi\xi'} = \theta_a^{\xi} - \theta_b^{\xi'}. \tag{4.21}$$

Eqs. (4.20), (4.21) represent the XY Mattis model, which is well known in the theory of spin glasses[65]. One can gauge out θ_a reducing Eq. (4.20) to a conventional form familiar from the s-wave superconductor or XY ferromagnet cases

$$E_J = -\frac{1}{2}\sum_{a\neq b} E_{ab}^{\xi\xi'} = -\frac{1}{2}\sum_{a\neq b} J_{ab}^{\xi\xi'} \cos\left(\tilde{\phi}_a^{\xi} - \tilde{\phi}_b^{\xi'}\right), \tag{4.22}$$

where $\tilde{\phi}_a^{\xi} = \phi_a + \theta_a^{\xi}$. Therefore the system is not a superconducting glass because its ground state has a hidden symmetry. In other words the Josephson coupling between islands inevitably favors globally a s-wave superconductivity, even though the order parameter on each island is unconventional. The system behaves as an s-wave superconductor with respect to all superconducting interference experiments. For example, corner squid experiments will not exhibit trapped fluxes. In the case where clean samples are in $p_x \pm ip_y$ state, the disordered samples will not have edge currents, and in the presence of the external magnetic field the order parameter will have conventional vortex structure familiar from the case of the s-wave superconductors.

Although our conclusions are quite general, for simplicity we consider the situation where the characteristic radius of the grain is of order of the zero temperature superconducting coherence length and the value of the order parameter in the puddles is much smaller than that in pure bulk superconductors, $|\Delta| \ll |\Delta_0|$. Such a situation, for example, takes place near the point of the quantum superconductor-metal transition, where the typical distance between the superconducting grains is larger than their size, which is of order the zero temperature coherence length. [66] In this case, at large separations between the grains, the Josephson coupling energy can be written in the form

$$E_{ab}^{\xi\xi'} = \mathrm{Re}\left[e^{i(\phi_a-\phi_b)} Z_{ab}^{\xi\xi'}\right], \tag{4.23}$$

where $Z_{ab}^{\xi\xi'}$ is given by

$$Z_{ab}^{\xi\xi'} = \mathrm{tr}\int d\mathbf{r}d\mathbf{r}'d\mathbf{p}d\mathbf{p}'\hat{\Delta}_a^{\xi}(\mathbf{r},\mathbf{p})\hat{C}(\mathbf{r}-\mathbf{r}';\mathbf{p},\mathbf{p}')\hat{\Delta}_b^{\xi'\dagger}(\mathbf{r}',\mathbf{p}'). \tag{4.24}$$

Here tr denotes the trace over all spin indices, and $\hat{C}(\mathbf{r}-\mathbf{r}';\mathbf{p},\mathbf{p}')$ is the integral of the Cooperon diagrams illustrated in Fig. 4.2 over energies. The exchange energies $J_{ab}^{\xi\xi'}$ and the phases θ_a^{ξ} are related to the modulus and phase of $Z_{ab}^{\xi\xi'} = J_{ab}^{\xi\xi'} \exp\left(i\left[\theta_a^{\xi} - \theta_b^{\xi'}\right]\right)$.

4.4.3 singlet pairing

Let us begin by considering the case where the Cooper pairing occurs in the singlet channel $\hat{\Delta}_a^{\xi} = i\hat{\sigma}_2\Delta_a^{\xi}(\mathbf{r},\mathbf{p})$, which includes s and d-wave superconductors. In the presence of disorder, even in the case where the clean bulk phase is a pure d-wave superconductor, the order parameter in each grain will contain an s-wave component

$$\Delta_a^{\xi}(\mathbf{r},\mathbf{p}) = \Delta_a^{(s),\xi}(\mathbf{r},\mathbf{p}) + \Delta_a^{(d),\xi}(\mathbf{r},\mathbf{p}). \tag{4.25}$$

where upper script in the parenthesis stands for the orbital symmetry whereas ξ and ξ' indicate Ising symmetry coming from time reversal invariance. Substituting Eq. (4.25) into Eq. (4.24) and evaluating the Cooperon we get three terms corresponding to s-s, s-d, and d-d Josephson coupling

$$Z_{ab}^{\xi\xi'} = Z_{ab}^{(ss),\xi\xi'} + Z_{ab}^{(dd),\xi\xi'} + Z_{ab}^{(sd),\xi\xi'}. \tag{4.26}$$

The s-s component is given by

$$Z_{ab}^{(ss),\xi\xi'} \propto \frac{\nu}{|\mathbf{r}_a - \mathbf{r}_b|^d} \langle\Delta_a^{\xi}\rangle\langle\Delta_b^{\xi'*}\rangle, \tag{4.27}$$

where ν is the density of states at the Fermi level, d is dimensionality of the system, $\mathbf{r}_a$ and $\mathbf{r}_b$ are the locations of grains a and b, and $\langle\Delta_a^{\xi}(\mathbf{r},\mathbf{p})\rangle$ denotes the order parameter integrated over the single grain,

$$\langle\Delta_a^{\xi}\rangle = \int d\mathbf{r}d\mathbf{p}\Delta_a^{\xi}(\mathbf{r},\mathbf{p}). \tag{4.28}$$

Strictly speaking, the slow power law decay of the Josephson coupling constant in Eq. (4.27) leads to a logarithmic divergence of the ground state energy. However, multiple Andreev reflections of diffusing electrons from the grains provide a cutoff of this divergence at distances of order $L_\Delta \sim r(r/r_p)^{(d-1)/2}(|\Delta_0|/|\Delta|)$[66]. Here $r_p \sim l$ is a typical superconducting puddle, r is typical intergrain distance, Δ_0 is a value of the order parameter in the bulk

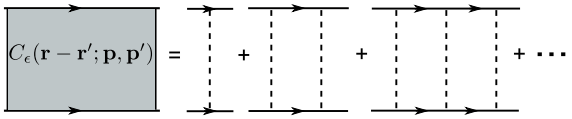

Figure 4.2: Diagrammatic representation of the Cooperon ladder. Solid lines are electron Green's functions whereas dashed lines are impurities. $\hat{C}(\mathbf{r}-\mathbf{r}';\mathbf{p},\mathbf{p})$ in Eq. (4.24) is obtained by integration of this ladder over energy.

superconductor, Δ is a typical value of the order parameter in a grain, and we assumed that the order parameter in different puddles have different phases. Since this length is greater than the typical distance between the grains our results are not affected by the presence of the cutoff.

The s-d and d-d contributions are given by

$$Z_{ab}^{(ds),\xi\xi'} \propto \nu \langle \Delta_b^{\xi' *} \rangle Q_{ij}^{a,\xi} \partial_i \partial_j \frac{1}{|\mathbf{r}_a - \mathbf{r}_b|^d}, \tag{4.29}$$

and

$$Z_{ab}^{(dd),\xi\xi'} \propto \nu\, Q_{a,ij}^{\xi} Q_{b,kl}^{\xi' \dagger} \partial_i \partial_j \partial_k \partial_l \frac{1}{|\mathbf{r}_a - \mathbf{r}_b|^d}. \tag{4.30}$$

In the above formulas the d-wave component of the order parameter in grain a is described by the second rank tensor $Q_{a,ij}^{\xi}$. For example for a spherical Fermi surface in which $\Delta^{(d),\xi}(\mathbf{r},\mathbf{p}) = Q_{a,ij}^{\xi}(\mathbf{r}) p_i p_j$ (with $Q_{ii}^{a}(\mathbf{r}) = 0$) we have

$$Q_{a,ij}^{\xi} = \int d\mathbf{r} Q_{a,ij}^{\xi}(\mathbf{r}). \tag{4.31}$$

It is important to note that the $Z_{ab}^{(sd)}$ and $Z_{ab}^{(dd)}$ fall off faster with the distance between the grains than $Z_{ab}^{(ss)}$. Therefore at large inter-grain separations they can be neglected. The leading term $Z_{ab}^{(ss)}$ given by Eq. (4.27) has a phase factor that can be written as a product of phase factors of individual grains which are independent of the direction of the link $\mathbf{r}_a - \mathbf{r}_b$. Therefore we arrive at the Mattis model, Eqs. (4.20) and (4.21), where θ_a^{ξ} is the phase of $\langle \Delta_a^{\xi} \rangle$ in Eq. (4.28).

4.4.4 triplet pairing

Let us now turn to triplet superconductivity. Even in the case where the clean bulk phase corresponds to $p_x + ip_y$ superconductivity, in a particular grain the order parameter will acquire an admixture of other p-wave components. However, in the absence of spin-orbit interactions the triplet and singlet components of the order parameter do not mix. In this case we get from Eq. (4.24) the following form of the Josephson coupling,

$$Z_{ab}^{(pp)} \propto \nu\, A_{a,i}^{\alpha} A_{b,j}^{\alpha *} \partial_i \partial_j \frac{1}{|\mathbf{r}_a - \mathbf{r}_b|^d}, \tag{4.32}$$

where the matrix $A_{a,i}^{\alpha}$ describes the p-wave order parameter in grain a. For example, for a spherical Fermi surface where $\hat{\Delta}_a(\mathbf{r}, \mathbf{p}) = \hat{\sigma}_\alpha A_{a,i}^{\alpha}(\mathbf{r}) p_i$ it is given by

$$A_{a,i}^{\alpha} = \int d\mathbf{r} A_{a,i}^{\alpha}(\mathbf{r}). \tag{4.33}$$

The phase of the Josephson coupling in Eq. (4.32) depends on the relative orientation between the spatial structure of the order parameter $A_{i\alpha}^{a}$ (which is characterized by the index i) and the direction of the bond between the grains. As a result the phase of $Z_{ab}^{(pp)}$ in Eq. (4.32) cannot be represented in the form of Eq. (4.21) in which the phases θ_a and θ_b depend only on the grain properties but not on the direction of the link connecting them, $\mathbf{r}_a - \mathbf{r}_b$. This means that we obtain the Josephson junction array with frustration.

However, in the presence of spin-orbit interactions in non-uniform superconductors the singlet, Δ, and triplet, $\mathbf{\Delta}$, component of the order parameter mix. In this case, at large separations between the grains the Josephson coupling is dominated by the s-wave component of the order parameter and is described by Eq. (4.27), which again leads us to the Mattis model, Eqs. (4.20), (4.21).

4.5 Consequence of corrections to Mattis model and global phase diagram

We have shown that at sufficiently strong disorder the properties of disordered unconventional superconductors at long spatial scales may be described by the model, Eq. (4.20). To leading order in the inter-grain distance the latter reduces to the Mattis model (4.22). We also obtained the leading corrections to the Mattis model approximation. Let us now discuss the physical consequences of these corrections.

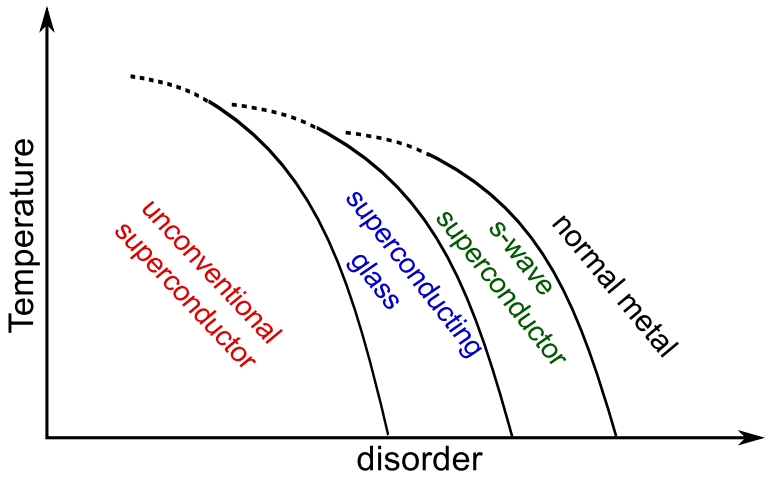

Figure 4.3: Schematic picture of the phase diagram of an unconventional superconductor as a function of temperature and disorder

We note that in the Mattis model approximation the values of $J_{ab}^{\xi\xi'}$ given by Eq. (4.27) are independent of the pseudo-spin variables ξ and ξ', which characterize the order parameters in individual grains. Therefore in this approximation the energy of the system is infinitely degenerate. The leading correction to the Josephson coupling energies have the form of **either Eq. (4.29) or (4.32).** In the presence of these corrections the expression for the energy of the system cannot be reduced to the Mattis model and acquires the form $\sum_{ab} J_{ab} \cos(\tilde{\phi}_a - \tilde{\phi}_b + \tilde{\theta}_{ab})$. Although the random phases $\tilde{\theta}_{ab}$ are small,

$$\tilde{\theta}_{ab}^{\xi\xi'} = \mathrm{Im} \ln \frac{Z_{ab}^{(pp),\xi\xi'}}{Z_{ab}^{(ss),\xi\xi'}} \ll 1,$$

they can not be decomposed according to Eq. (4.21). One important consequence of the corrections to the Mattis model is that they lift the energy degeneracy of the system with respect to the pseudo-spin variables ξ. Thus the subsystem of pseudo-spins forms a glass state. Another consequence of the corrections is that they produce currents in the ground state of the system. In the three dimensional case existence of the corrections to the Mattis model do not destroy the long range order of the order parameter characterized by the phase $\tilde{\phi}$. Therefore the conclusion about the s-wave-like nature of the superconducting interference experiments remains correct. In two spatial dimensions the corrections terms

do destroy the long range order since the correlation function of the phases in the ground state diverges logarithmically at large distances. However, as long as $\tilde{\theta}_{ab}^{\xi\xi'} \ll 1$, the length at which the phase changes by a number of order unity is exponentially large in comparison to the inter-grain distance.

At intermediate strength of disorder when the distance between the superconducting islands is of order their size, the effective energy of the system, Eq. (4.20), cannot be reduced to the Mattis model, Eq. (4.22). The phases $\tilde{\theta}_{ab}$ that cause frustration are of order unity. In this case the system is a superconducting glass.[61, 62]. The global phase diagram of the system is schematically shown in Fig. 4.3.

BIBLIOGRAPHY

[1] Andrew Peter Mackenzie and Yoshiteru Maeno. The superconductivity of Sr_2RuO_4 and the physics of spin-triplet pairing. *Rev. Mod. Phys.*, 75:657–712, May 2003.

[2] John Bardeen, Leon N Cooper, and J Robert Schrieffer. Theory of superconductivity. *Physical Review*, 108(5):1175, 1957.

[3] HEIKE Kamerlingh Onnes. Investigations into the properties of substances at low temperatures, which have led, amongst other things, to the preparation of liquid helium. *Nobel lecture*, 4, 1913.

[4] P de Gennes. *Superconductivity of metals and alloys*. Addison-Wesley New York, 1989.

[5] Michael Tinkham. *Introduction to superconductivity*. Courier Dover Publications, 2012.

[6] J.R. Schrieffer. *Theory of superconductivity*. Addison-Wesley, 1964.

[7] VP Mineev and KV Samokhin. *Introduction to Unconventional Superconductivity*. Gordon and Breach, Amsterdam, 1999.

[8] Toshihiko Tsuneto. *Superconductivity and superfluidity*. Cambridge University Press, 2005.

[9] NN Bogoliubov. *Soviet Phys. JETP*, 34:41, 1958.

[10] JG Valatin. Comments on the theory of superconductivity. *Il Nuovo Cimento*, 7(6):843–857, 1958.

[11] L.P. Gor'kov. *Soviet Phys. JETP*, 7:505, 1958.

[12] Yoichiro Nambu. Quasi-particles and gauge invariance in the theory of superconductivity. *Phys. Rev.*, 117:648–663, Feb 1960.

[13] Lev Petrovich Gorkov. Microscopic derivation of the ginzburg-landau equations in the theory of superconductivity. *Sov. Phys. JETP*, 9(6):1364–1367, 1959.

[14] P. W. Anderson and P. Morel. Generalized bardeen-cooper-schrieffer states and the proposed low-temperature phase of liquid ^{3}He. *Phys. Rev.*, 123:1911–1934, Sep 1961.

[15] G. R. Stewart. Heavy-fermion systems. *Rev. Mod. Phys.*, 56:755–787, Oct 1984.

[16] J George Bednorz and K Alex Müller. Possible hight c superconductivity in the ba-la- cu- o system. *Zeitschrift für Physik B Condensed Matter*, 64(2):189–193, 1986.

[17] TM Rice and M Sigrist. Sr2ruo4: an electronic analogue of 3he? *Journal of Physics: Condensed Matter*, 7(47):L643, 1995.

[18] Philip W Anderson. Theory of dirty superconductors. *Journal of Physics and Chemistry of Solids*, 11(1):26–30, 1959.

[19] Alexei A Abrikosov and L.P. Gor'kov. *Sov. Phys. JETP*, 8(1090), 1959.

[20] Yoshiteru Maeno, Shunichiro Kittaka, Takuji Nomura, Shingo Yonezawa, and Kenji Ishida. Evaluation of spin-triplet superconductivity in Sr_2RuO_4. *arXiv preprint arXiv:1112.1620*, 2011.

[21] Jing Xia, Yoshiteru Maeno, Peter T. Beyersdorf, M. M. Fejer, and Aharon Kapitulnik. High resolution polar kerr effect measurements of Sr_2RuO_4: Evidence for broken time-reversal symmetry in the superconducting state. *Phys. Rev. Lett.*, 97:167002, Oct 2006.

[22] Catherine Kallin. Chiral p-wave order in sr2ruo4. *Reports on Progress in Physics*, 75(4):042501, 2012.

[23] JR Kirtley, C Kallin, CW Hicks, E-A Kim, Ying Liu, KA Moler, Y Maeno, and KD Nelson. Upper limit on spontaneous supercurrents in Sr_2RuO_4. *Physical Review B*, 76(1):014526, 2007.

[24] Michael Stone and Inaki Anduaga. Mass flows and angular momentum density for $p_x + ip_y$ paired fermions in a harmonic trap. *Annals of Physics*, 323(1):2–16, 2008.

[25] S. Raghu, A. Kapitulnik, and S. A. Kivelson. Hidden quasi-one-dimensional superconductivity in sr_2ruo_4. *Phys. Rev. Lett.*, 105:136401, Sep 2010.

[26] A.A. Abrikosov, Lev Petrovich Gorkov, and Igor Ekhielevich Dzyaloshinski. *Methods of quantum field theory in statistical physics*. Courier Dover Publications, 2012.

[27] Manfred Sigrist and Kazuo Ueda. Phenomenological theory of unconventional superconductivity. *Rev. Mod. Phys.*, 63:239–311, Apr 1991.

[28] P. W. Anderson. Random-phase approximation in the theory of superconductivity. *Phys. Rev.*, 112:1900–1916, Dec 1958.

[29] EM Lifshitz and LP Pitaevskii. Statistical physics part 2, Landau and Lifshitz course of theoretical physics, 1980.

[30] LV Keldysh. Diagram technique for nonequilibrium processes. *Sov. Phys. JETP*, 20(4):1018–1026, 1965.

[31] LP Pitaevskii and EM Lifshitz. *Physical kinetics*, volume 10. Butterworth-Heinemann, 1981.

[32] JW Serene and Dierk Rainer. The quasiclassical approach to superfluid ^{3}He. *Physics Reports*, 101(4):221–311, 1983.

[33] J. Rammer and H. Smith. Quantum field-theoretical methods in transport theory of metals. *Rev. Mod. Phys.*, 58:323–359, Apr 1986.

[34] AI Larkin and YUN Ovchinnikov. Nonlinear conductivity of superconductors in the mixed state. *Sov. Phys. JETP*, 41(5):960–965, 1975.

[35] AI Larkin and YUN Ovchinnikov. Non-linear effects during the motion of vortices in superconductors. *Sov. Phys. JETP*, 46(1):155, 1977.

[36] AI Larkin and Yu N Ovchinnikov. Quasiclassical method in the theory of superconductivity. *SOV PHYS JETP*, 28(6):1200–1205, 1969.

[37] Gert Eilenberger. Transformation of gorkov's equation for type ii superconductors into transport-like equations. *Zeitschrift für Physik*, 214(2):195–213, 1968.

[38] Ulrich Eckern. Quasiclassical approach to kinetic equations for superfluid 3hellum: General theory and application to the spin dynamics. *Annals of Physics*, 133(2):390–428, May 1981.

[39] Klaus D. Usadel. Generalized Diffusion Equation for Superconducting Alloys. *Physical Review Letters*, 25(8):507–509, August 1970.

[40] AV Zaitsev. Quasiclassical equations of the theory of superconductivity for contiguous metals and the properties of constricted microcontacts. *Zh. Eksp. Teor. Fiz*, 86:1742–1758, 1984.

[41] M Yu Kuprianov and VF Lukichev. Influence of boundary transparency on the critical current of dirty SS'S structures. *Zh. Eksp. Teor. Fiz*, 94:149, 1988.

[42] A Millis, D Rainer, and JA Sauls. Quasiclassical theory of superconductivity near magnetically active interfaces. *Physical Review B*, 38(7):4504, 1988.

[43] G. E. Blonder, M. Tinkham, and T. M. Klapwijk. Transition from metallic to tunneling regimes in superconducting microconstrictions: Excess current, charge imbalance, and supercurrent conversion. *Phys. Rev. B*, 25:4515–4532, Apr 1982.

[44] F. W. J. Hekking and Yu. V. Nazarov. Subgap conductivity of a superconductor-normal-metal tunnel interface. *Phys. Rev. B*, 49:6847–6852, Mar 1994.

[45] T. H. Stoof and Yu. V. Nazarov. Kinetic-equation approach to diffusive superconducting hybrid devices. *Phys. Rev. B*, 53:14496–14505, Jun 1996.

[46] C. W. J. Beenakker. Quantum transport in semiconductor-superconductor microjunctions. *Phys. Rev. B*, 46:12841–12844, Nov 1992.

[47] C. W. J. Beenakker. Random-matrix theory of quantum transport. *Rev. Mod. Phys.*, 69:731–808, Jul 1997.

[48] Fei Zhou, B. Spivak, and A. Zyuzin. Coherence effects in a normal-metal-insulator-superconductor junction. *Phys. Rev. B*, 52:4467–4472, Aug 1995.

[49] K. D. Nelson, Z. Q. Mao, Y. Maeno, and Y. Liu. Odd-parity superconductivity in Sr_2RuO_4. *Science*, 306(5699):1151–1154, 2004.

[50] Francoise Kidwingira, J. D. Strand, D. J. Van Harlingen, and Yoshiteru Maeno. Dynamical superconducting order parameter domains in Sr_2RuO_4. *Science*, 314(5803):1267–1271, 2006.

[51] GM Luke, Y Fudamoto, KM Kojima, MI Larkin, J Merrin, B Nachumi, YJ Uemura, Y Maeno, ZQ Mao, Y Mori, et al. Time-reversal symmetry-breaking superconductivity in Sr_2RuO_4. *Nature*, 394(6693):558–561, 1998.

[52] Satoshi Kashiwaya, Hiromi Kashiwaya, Hiroshi Kambara, Tsuyoshi Furuta, Hiroshi Yaguchi, Yukio Tanaka, and Yoshiteru Maeno. Edge states of sr_2ruo_4 detected by in-plane tunneling spectroscopy. *Phys. Rev. Lett.*, 107:077003, Aug 2011.

[53] F. Laube, G. Goll, H. v. Löhneysen, M. Fogelström, and F. Lichtenberg. Spin-triplet superconductivity in sr2ruo4 probed by andreev reflection. *Phys. Rev. Lett.*, 84:1595–1598, Feb 2000.

[54] Y Liu, KD Nelson, ZQ Mao, R Jin, and Y Maeno. Tunneling and phase-sensitive studies of the pairing symmetry in sr2ruo4. *Journal of low temperature physics*, 131(5-6):1059–1068, 2003.

[55] H Murakawa, K Ishida, K Kitagawa, ZQ Mao, and Y Maeno. Measurement of the Ru 101-knight shift of superconducting Sr_2RuO_4 in a parallel magnetic field. *Physical review letters*, 93(16):167004, 2004.

[56] AL Shelankov. On the derivation of quasiclassical equations for superconductors. *Journal of low temperature physics*, 60(1-2):29–44, 1985.

[57] F Zhou and B Spivak. Hall effect in sn and sns junctions. *Physical Review Letters*, 80(17):3847, 1998.

[58] G.E Volovik and L.P. Gor'kov. *JETP Lett.*, 39(674), 1984.

[59] M. Sigrist and K. Ueda. *Rev. Mod. Phys.*, 63(239), 1991.

[60] C. C. Tsuei and J. R. Kirtley. *Rev. Mod. Phys.*, 72(969), 2000.

[61] S. Kivelson B. Spivak. *Physics B*, 404(462), 2009.

[62] P. Oreto B. Spivak and S. Kivelson. *Phys. Rev B*, 77(214523), 2008.

[63] AP Mackenzie, RKW Haselwimmer, AW Tyler, GG Lonzarich, Y Mori, S Nishizaki, and Y Maeno. Extremely strong dependence of superconductivity on disorder in sr 2 ruo 4. *Physical review letters*, 80(1):161, 1998.

[64] A. F. Andreev. *Sov. Phys. JETP*, 19(1228), 1964.

[65] DC Mattis. *Physics Letters A*, 56(421), 1976.

[66] B. Spivak, A. Zyuzin, and M. Hruska. *Phys. Rev. B*, 64(132502), 2001.

[67] Michael Tinkham. *Introduction to superconductivity*. Courier Dover Publications, 2012.

[68] Takafumi Kita. The angular momentum paradox of $^3He - A$. *Journal of the Physical Society of Japan*, 65(3):664–666, 1996.

[69] Y Tanaka, Yu V Nazarov, AA Golubov, and S Kashiwaya. Theory of charge transport in diffusive normal metal/unconventional singlet superconductor contacts. *Physical Review B*, 69(14):144519, 2004.

[70] B Spivak, P Oreto, and SA Kivelson. d-wave to s-wave to normal metal transitions in disordered superconductors. *Physica B: Condensed Matter*, 404(3):462–465, 2009.

[71] Alfonso Romano, Paola Gentile, Canio Noce, Ilya Vekhter, and Mario Cuoco. Magnetic intragap states and mixed parity pairing at the edge of spin-triplet superconductors. *Physical review letters*, 110(26):267002, 2013.

[72] Wolfgang Belzig, Frank K Wilhelm, Christoph Bruder, Gerd Schön, and Andrei D Zaikin. Quasiclassical Greens function approach to mesoscopic superconductivity. *Superlattices and Microstructures*, 25(5-6):1251–1288, May 1999.

[73] Karl-Heinz Bennemann and John B Ketterson. *The Physics of Superconductors: Vol. II: Superconductivity in Nanostructures, High-Tc and Novel Superconductors, Organic Superconductors*. Springer, 2004.

[74] C J Lambert and R Raimondi. Phase-coherent transport in hybrid superconducting nanostructures. *Journal of Physics: Condensed Matter*, 10(5):901–941, February 1998.

[75] P.W. Anderson. Theory of dirty superconductors. *Journal of Physics and Chemistry of Solids*, 11(1-2):26–30, September 1959.

[76] Leon N Cooper and Dmitri Feldman. *BCS: 50 years*. World scientific, 2011.

[77] Cliffird W. Hicks et. al. *Science*, 344(283), 2014.